

# Oxytocin modulates social value representations in the amygdala

Yunzhe Liu<sup>1,2,3</sup>, Shiyi Li<sup>1,2,3,7</sup>, Wanjun Lin<sup>1,2,3,7</sup>, Wenxin Li<sup>4,7</sup>, Xinyuan Yan<sup>1,2,3</sup>, Xuena Wang<sup>4</sup>, Xinyue Pan<sup>4</sup>, Robb B. Rutledge<sup>5,6</sup> and Yina Ma<sup>1,2,3\*</sup>

**Humans exhibit considerable variation in how they value their own interest relative to the interests of others. Deciphering the neural codes representing potential rewards for self and others is crucial for understanding social decision-making. Here we integrate computational modeling with functional magnetic resonance imaging to investigate the neural representation of social value and the modulation by oxytocin, a nine-amino acid neuropeptide, in participants evaluating monetary allocations to self and other (self–other allocations). We found that an individual's preferred self–other allocation serves as a reference point for computing the value of potential self–other allocations. In more prosocial participants, amygdala activity encoded a social-value-distance signal; that is, the value dissimilarity between potential and preferred allocations. Intranasal oxytocin administration amplified this amygdala representation and increased prosocial behavior in more individualistic participants but not in more prosocial ones. Our results reveal a neurocomputational mechanism underlying social-value representations and suggest that oxytocin may promote prosociality by modulating social-value representations in the amygdala.**

Humans live in complex social environments and rely heavily on social reciprocity. Many of our important decisions are made in social contexts where the costs and benefits to both ourselves and other people need to be considered<sup>1</sup>. Deciphering the neural codes that represent potential rewards to oneself and others is crucial for understanding social reciprocity and social decisions<sup>2</sup>. Recent studies of social decision-making find that people are rarely purely self-centered or altruistic: they care about both themselves and others' interests, but with considerable individual variation in how they weigh equity of self–other gain<sup>3</sup> and cooperation with others<sup>3,4</sup> during their decision-making. Individuals with prosocial preferences tend to prefer allocations considering the interests of both self and other and often seek to minimize the self–other difference (henceforth, prosocials). In contrast, individuals with selfish preferences tend to maximize resources for themselves and generally prefer self-centered allocations (henceforth, individualists).

Individual differences in social preference may stem from individual variation in preferred social allocations and differences in neural representations of potential relative to preferred allocations<sup>5–7</sup>. It remains unclear how the difference between potential and preferred self–other allocations is computed and represented in the brain, and how these computations and neural representations are related to social decision-making. Here, we propose that the preferred self–other allocation (that is, what an individual hopes the allocation will be) serves as a social reference point against which potential allocations are represented and that quantity can guide social value-based decisions (social reference model). The deviation from the preferred allocation generates an 'error' signal that could drive adaptive actions to reduce the size of the deviation. In much the same way as reward prediction errors<sup>8</sup> represent differences between expected and actual rewards and provide a basis for value-based decisions<sup>9,10</sup>, this social error signal could represent deviation

from the preferred allocation and serve as a basis for value-based decisions in the social domain.

The amygdala, with oxytocin and dopamine receptors<sup>11,12</sup> and strongly implicated in social cognition and social decision-making<sup>3,13</sup>, is a prominent candidate to encode deviations from a social reference point. Recent studies have shown that amygdala activity tracks the subjective values of rewards and punishments<sup>14</sup> and reflects individual preferences<sup>15</sup>. Notably, the amygdala has been suggested to encode error signals that represent the differences between expectations and outcomes<sup>9</sup>, a quantity that is fundamental for value-based decision-making<sup>2</sup>. Amygdala activity has also been shown to encode 'aversive' signals to absolute inequality when evaluating reward pairs for self and other<sup>3</sup> and in response to dishonest behavior<sup>16</sup>. One untested possibility is that amygdala activity encodes the deviation of a potential self–other allocation from a reference point that depends on individual-specific social preferences.

Prosocials and individualists, who should differ in their social reference point, would be expected to engage different neural substrates for social value representations. For prosocials, the distance from their social reference point could signal deviation from normative social principles such as inequity aversion, which is associated with the amygdala<sup>3</sup>. On the other hand, individualists employing a self-interest maximizing strategy in their decision-making could represent deviation from this reference point mainly as conflict with self-interest, engaging lateral prefrontal regions associated with inhibition of self-interest and self–other allocation trade-off<sup>17</sup>, such as lateral orbitofrontal cortex (IOFC)<sup>18,19</sup> and dorsolateral prefrontal cortex (dlPFC)<sup>20</sup>.

It has also been suggested that individual differences in social behavior result in part from differences in the neuromodulatory regulation of neural circuits<sup>6</sup>. The neuropeptide oxytocin, an evolutionarily conserved hormone, is a potential candidate<sup>21</sup>. Oxytocin

<sup>1</sup>State Key Laboratory of Cognitive Neuroscience and Learning, Beijing Normal University, Beijing, China. <sup>2</sup>IDG/McGovern Institute for Brain Research, Beijing Normal University, Beijing, China. <sup>3</sup>Beijing Key Laboratory of Brain Imaging and Connectomics, Beijing Normal University, Beijing, China. <sup>4</sup>School of Psychological and Cognitive Sciences, Peking University, Beijing, China. <sup>5</sup>Wellcome Centre for Human Neuroimaging, University College London, London, UK. <sup>6</sup>Max Planck University College London Centre for Computational Psychiatry and Ageing Research, University College London, London, UK.

<sup>7</sup>These authors contributed equally: Shiyi Li, Wanjun Lin and Wenxin Li. \*e-mail: [yina.ma@bnu.edu.cn](mailto:yina.ma@bnu.edu.cn)

has been found to play an important role in social interaction and social decision-making<sup>22</sup>, including promoting social motivation<sup>23</sup>, increasing trust and cooperation with own-group members<sup>24</sup> and reducing social distance<sup>25</sup>. Whether and how oxytocin modulates the basic computations of social preference and social value representations remains largely unexplored. Individual differences in social preferences in nonhuman primates have been shown to be due in part to oxytocinergic regulation of amygdala-related neural circuits<sup>6,7</sup>. In nonhuman primates, exogenous inhaled oxytocin promotes social donation behavior<sup>26</sup> and focal infusion of oxytocin into the amygdala significantly increases prosocial decisions<sup>7</sup>. In humans, it has been suggested that individual differences in oxytocin effects are adaptive depending on an individual's social disposition<sup>21</sup> such that intranasal oxytocin produces stronger effects on cooperation in less socially proficient individuals<sup>4</sup>. Oxytocin differentially affects cooperative and aggressive choices in individuals with different pre-existing beliefs in prosociality<sup>27</sup>. We therefore predicted differential effects of oxytocin on regulating prosocial behavior between prosocials and individualists by selectively increasing prosociality in individualists via amplification of amygdala social value representations.

Here, we set out to test whether intranasal administration of oxytocin differentially modulates the neural representation of social values in prosocials and individualists performing a monetary outcome-pair evaluation task during functional magnetic resonance imaging (fMRI) scanning in a double-blind placebo-controlled between-subjects design. We first show that our social reference model most parsimoniously explains behavior consistent with social values being encoded as distance to an individual-specific reference point. While prosocials represent social values relative to a more prosocial reference point than individualists, oxytocin selectively increased prosociality in individualists and not prosocials in both competitive and non-competitive contexts. Moreover, these findings were replicated in two additional behavioral experiments. Using model-based fMRI analysis, we found that under placebo, amygdala activity in prosocials encodes a social value distance reflecting the degree to which a potential self-other allocation deviates from an individual-specific reference point. Oxytocin selectively amplified the neural representation of social values in the amygdala in individualists, suggesting a link between oxytocin and prosociality via modulation of social value representations in the amygdala.

## Results

**Experimental settings.** In the fMRI experiment, we first invited participants ( $n = 282$ ) to a behavioral session to identify their social dispositions (that is, prosocials versus individualists) using the triple dominance<sup>5</sup> and social value orientation (SVO)<sup>28</sup> decision-making tasks (Supplementary Fig. 1). Thereafter, eligible prosocials and individualists ( $n = 127$ ) administered oxytocin or placebo performed a monetary outcome-pair evaluation task during fMRI scanning (Fig. 1a). On each trial, participants were presented with pairs of monetary outcomes for himself and another participant (referred to as the partner) and evaluated his preference on each pair.

All monetary allocations were evenly sampled on the circumference of a circle centered at the origin (0, 0) in the Cartesian coordinate space spanned by social values (with monetary outcomes for self as the  $x$  axis and outcomes for the partner as the  $y$  axis, radius, 5, Fig. 1a). Monetary outcomes for oneself and the partner define an angle  $\theta$ , which samples the space from  $-90^\circ$  to  $180^\circ$ . The angle between any two potential allocations is both necessary and sufficient to quantify their relationship. Both positive and negative values were included for a comprehensive investigation of social value representations, except for those in the third quadrant due to invariant preference rating shown in an independent sample (Methods).

We also ran two additional behavioral experiments, one experiment with a large sample (behavioral online-replication experi-

ment,  $n = 315$ ) providing a replication for our finding that the social reference model outperforms other models and one experiment providing a replication of the oxytocin effect (oxytocin-replication experiment,  $n = 80$  males, within-subjects design, 40 prosocials and 40 individualists). To improve the ability to distinguish between different models, both additional experiments were run on a modified design where monetary pairs were sampled on three circles of different circumference (radius of 5, 6, 9), with  $\theta$  ranging from  $-90^\circ$  to  $180^\circ$  with different intervals ( $5^\circ$ ,  $17^\circ$ ,  $23^\circ$ ). These specifications were identified based on model recovery analysis, which suggested that the combination of these parameters would lead to maximal discriminability between our social reference model and an inequality aversion model. The task design for these additional experiments was otherwise identical to the fMRI experiment.

**Representing social values according to an individual-specific reference point.** In the fMRI experiment, we first plotted  $z$ -scored preference ratings for each self-other allocation across participants for visualization purposes (Fig. 1b). In general, participants most preferred self-gain/other-gain pairs and least preferred self-loss/other-gain pairs, suggesting that they considered the interests of both self and the partner. Based on preference ratings for all allocations, we computed an individual-specific reference point,  $\varphi$ . The principle of  $\varphi$  calculation was consistent with the 'mean orientation' measure in a map-like structure<sup>29,30</sup> (Fig. 1c). The degree of  $\varphi$  indicated how much a participant preferred the potential outcome for the partner in relation to himself, with greater degree of  $\varphi$  corresponding to stronger preference for allocations that benefit the partner relative to oneself and thus greater prosociality.

We then calculated cosine similarity between each allocation  $\theta$  and the individual-specific  $\varphi$  to compute the social value distance, the dissimilarity distance of that allocation to the participant's preferred allocation (also the deviation from the social reference point, calculated as  $1 - \cos(\theta - \varphi)$ ). This measurement allowed us to quantify the difference between the second (self-loss/other-gain pairs) and fourth (self-gain/other-loss pairs) quadrants (Fig. 1c), which is not feasible when only including gains or using absolute value differences<sup>3,28</sup>. The social reference model was consistently the most parsimonious model across all studies: the fMRI during-scan experiment, the post-scan behavioral experiment, the behavioral online-replication experiment and the oxytocin-replication experiment (supported by model comparisons using variational free energy as the model selection criteria, see Supplementary Fig. 2).

**More prosocial reference points for social value representations in prosocials.** We quantified the difference in the estimated reference point between prosocials and individualists under placebo. We found significantly higher values of  $\varphi$  in prosocials than individualists ( $F(1,59) = 33.49$ ,  $P = 2.91 \times 10^{-7}$ ,  $\eta^2 = 0.36$ , Fig. 2a), which was replicated in the large sample online experiment ( $F(1,313) = 92.14$ ,  $P = 2.71 \times 10^{-19}$ ,  $\eta^2 = 0.23$ , Fig. 2b). Moreover, in the online-replication experiment, the social reference point derived from the social reference model was correlated with individuals' SVO scores ( $r = 0.55$ ,  $P = 4.38 \times 10^{-26}$ , 95% confidence interval (CI) = 0.47, 0.62, Fig. 2c), suggesting a more prosocial reference point in prosocials both at a group and individual level. The pattern of more prosocial reference points in prosocials than individualists was similarly observed in the competitive context in the post-scan experiment ( $F(1,59) = 12.59$ ,  $P = 7.69 \times 10^{-4}$ ,  $\eta^2 = 0.18$ , Fig. 2d) and in the oxytocin-replication experiment ( $F(1,78) = 28.27$ ,  $P = 9.78 \times 10^{-7}$ ,  $\eta^2 = 0.27$ , Fig. 2e).

Under placebo,  $\varphi$  was significantly correlated with independent measures of previously established prosocial behavior (Methods), with positive correlations between  $\varphi$  and the amount of contribution in a public goods game ( $r = 0.52$ ,  $P = 2.44 \times 10^{-5}$ ) and in a dictator

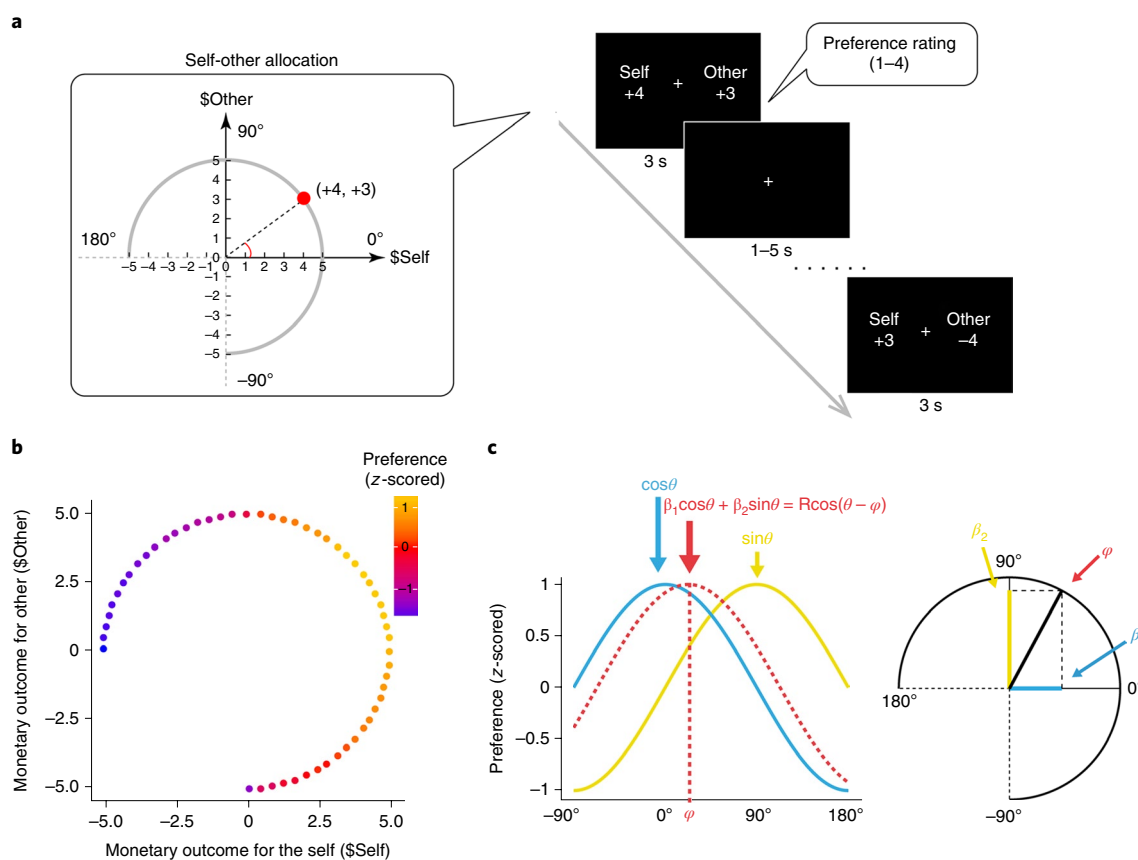


**Fig. 1 | Experimental design.** **a**, Participants were presented with monetary outcome pairs specifying potential amounts of money ('+' indicated gain and '-' indicated loss) received by themselves (self) and another player (other). Participants had 3 s to rate their preferences from 1 (least preferable) to 4 (most preferable) for each monetary outcome pair, followed by a 1–5 s jittered inter-trial interval. Monetary outcomes for the self and other define an angle  $\theta$ , which samples the space from  $-90^\circ$  to  $180^\circ$ . **b**, Mean standardized preference ratings across all participants were plotted against monetary allocations for the self and other. **c**, Based on the preference ratings, we computed the reference point in the social value representation  $\varphi$ , closely related to the preferred allocation that best accounts for the participants' social preferences over all allocations. Higher values of  $\varphi$  correspond to a stronger preference for allocations that benefit the partner relative to oneself, indicating greater prosociality.

game ( $r=0.44$ ,  $P=0.0006$ ). The degree of  $\varphi$  was also correlated with the degree of absolute inequality aversion (which reflected a general preference for fairness and resistance to inequalities, with higher values indicating higher inequality aversion,  $r=0.65$ ,  $P=1.54 \times 10^{-8}$ ), measured in an independent task<sup>28</sup> (Methods). Note that a  $\varphi$  of  $45^\circ$  indicates a preference for equal offers. In a fairly small range of  $\varphi$  corresponding to most of our participants ( $-30$  to  $45^\circ$ ), the larger the  $\varphi$ , the more prosocial a participant.

It has been suggested that decision time reflects perceived conflicts between prior expectation and current choice, with faster responses for preferred and less conflicted choices<sup>31,32</sup>. Thus, we would expect faster decision-making when conflict is minimal and the potential allocation is close to the individual-specific reference point. As the social value distance increased, longer decision times were predicted. We indeed found that decision time for a potential allocation increased as a function of deviation from an individual-specific reference point, and such a correlation was stronger in individualists than prosocials under placebo (independent-samples  $t$ -test on the Fisher  $z$ -scored correlation coefficients, individualists versus prosocials:  $0.18 \pm 0.03$  versus  $0.09 \pm 0.02$ ;  $t(59)=2.33$ ,  $P=0.023$  in the fMRI experiment, with a similar trend in the oxytocin-replication experiment, paired-samples  $t$ -test:  $t(78)=1.86$ ,  $P=0.067$ , Supplementary Fig. 3). The greater the dissimilarity between potential and preferred allocations, the longer individualists took to evaluate potential allocations.

**Selective oxytocin effects on promoting prosociality in individualists.** We evaluated the oxytocin effect on the social value representations. First, we checked the relationship between baseline salivary oxytocin and social value representations across all participants. The individual-specific reference point,  $\varphi$ , was independent of baseline salivary oxytocin ( $r=0.03$ ,  $P=0.75$ ) (Supplementary Fig. 4). We also measured participants' social perceptions of their partner by rating the first impression, likeability and attractiveness of the partner. There was no significant difference across all groups on any of these measures (Supplementary Fig. 5). Therefore, any significant effect of Social Disposition and/or Treatment on the social value representation cannot be attributed to baseline oxytocin or social perception differences.

We conducted analysis of variance (ANOVA) on  $\varphi$ , with Social Disposition (prosocials versus individualists) and Treatment (oxytocin versus placebo) as between-subjects factors. There was a significant main effect of Social Disposition ( $F(1,121)=28.09$ ,  $P=5.29 \times 10^{-7}$ ,  $\eta^2=0.19$ ), with prosocials (versus individualists) using a more prosocial reference point to evaluate potential allocations. We found a significant Social Disposition  $\times$  Treatment interaction ( $F(1,121)=6.35$ ,  $P=0.013$ ,  $\eta^2=0.05$ , Fig. 2a), as intranasal oxytocin significantly increased the reference point  $\varphi$  toward a preference for more prosocial allocations in individualists (independent-samples  $t$ -test,  $t(57)=2.21$ ,  $P=0.031$ ), but not in prosocials ( $t(64)=-1.54$ ,  $P=0.13$ , Fig. 2a), indicating that oxytocin



**Fig. 2 | Oxytocin boosts prosociality selectively in individualists. a–e**, More prosocial reference points for social value representations in prosocials than individualists in the fMRI during-scan experiment (**a**, 31 prosocials and 30 individualists,  $P = 2.91 \times 10^{-7}$ , under placebo), in the online-replication experiment (**b**,  $n = 315$ , 160 prosocials and 155 individualists,  $P = 2.71 \times 10^{-19}$ ), in the fMRI post-scan experiment (**d**, in a competitive context via framing the payoff in a winner-takes-all manner,  $P = 7.69 \times 10^{-4}$ , under placebo) and in the oxytocin-replication experiment (**e**, 40 prosocials and 40 individualists,  $P = 9.78 \times 10^{-7}$ , under placebo). In the online-replication experiment, the estimated social reference point was positively correlated with individual SVO scores: the more prosocial the disposition, the higher the  $\varphi$  (**c**,  $n = 315$ , Pearson's  $r = 0.55$ ,  $P = 4.38 \times 10^{-26}$ ). Moreover, intranasal oxytocin increased prosociality in individualists but not in prosocials, by moving their reference point  $\varphi$  toward a preference for more prosocial allocations in the fMRI during-scan experiment (**a**,  $n = 125$ , individualists under placebo:  $n = 30$  males, under oxytocin:  $n = 29$  males; prosocials under placebo:  $n = 31$  males, under oxytocin:  $n = 35$  males,  $P = 0.013$ ) and in the oxytocin-replication experiment (**e**,  $n = 40$  prosocials and 40 individualists,  $P = 0.011$ ). Moreover, in the oxytocin-replication experiment, SVO scores were negatively correlated with the effect of oxytocin on social reference point (**f**,  $n = 80$ , Pearson's  $r = -0.23$ ,  $P = 0.041$ ). The individual-specific  $\varphi < 0^\circ$  indicates a preference for pairs with self-gain and other-loss;  $\varphi = 0^\circ$  indicates a preference for self-gain without consideration of other's outcome;  $0^\circ < \varphi < 90^\circ$  indicates a preference for self-gain/other-gain pairs;  $\varphi > 90^\circ$  indicates a preference for self-loss/other-gain pairs). Error bars represented s.e.m. across participants in each group (\* $P < 0.05$ , \*\* $P < 0.01$  and \*\*\* $P < 0.001$ ; NS, not significant).

selectively increased prosociality in individualists. Furthermore, there was no effect of scanning order or partner type on  $\varphi$  (Supplementary Fig. 6).

We replicated the selective oxytocin effect on promoting prosociality in individualists in the independent oxytocin behavioral experiment where we employed a within-subjects design and included monetary pairs sampled on three circles of different circumferences (Social Disposition:  $F(1,78) = 19.51$ ,  $P = 3.19 \times 10^{-5}$ ,  $\eta^2 = 0.20$ ; Social Disposition by Treatment interaction:  $F(1,78) = 6.73$ ,  $P = 0.011$ ,  $\eta^2 = 0.079$ , Fig. 2e). Moreover, the within-subjects design, where each participant was invited to both oxytocin and placebo sessions, allowed us to examine whether the oxytocin effect varied as a function of individual scores in SVO. We expected a negative correlation between SVO scores and the oxytocin effect on prosociality, and indeed found a significant negative correlation between SVO scores and the size of oxytocin effect on social reference point ( $r = -0.23$ ,  $P = 0.041$ , Fig. 2f), suggesting that the more individualistic

the individual, the stronger the effect of oxytocin on promoting a prosocial reference point.

Finally, to determine whether the lack of oxytocin effect on prosocials was due to a ceiling effect (that is, prosocials already care about others' outcomes), we introduced a competitive social context in the post-scan behavioral task where self-interest and other-interest were in direct competition. In the competitive context, we framed the payoff in a 'winner takes all' manner, so that one would be motivated to make selfish decisions to gain more than the partner. If oxytocin can promote prosociality in prosocials, which is masked by a ceiling effect in the non-competitive setting, we would expect oxytocin to affect prosocials in the competitive context. We conducted an ANOVA on  $\varphi$  in prosocials, with Treatment as between-subjects factor and Context (competitive versus non-competitive) as within-subjects factor. There was a significant main effect of Context ( $F(1,64) = 68.61$ ,  $P = 1.02 \times 10^{-11}$ ,  $\eta^2 = 0.52$ ), but no Treatment effect ( $F(1,64) = 0.856$ ,  $P = 0.358$ ) or interaction

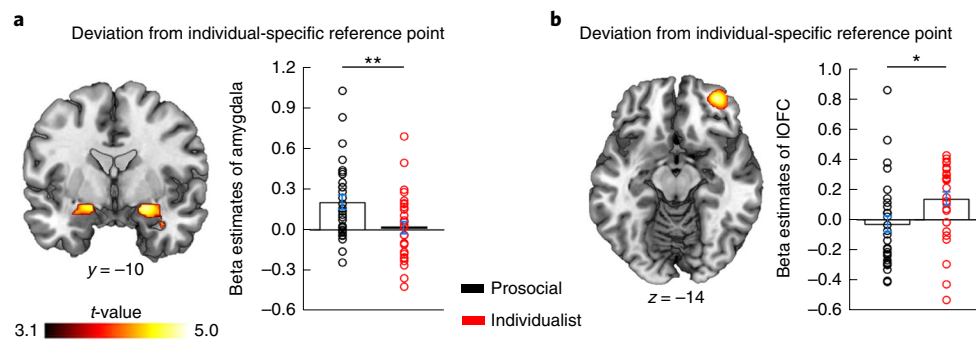


**Fig. 3 | Amygdala activity in prosocials ( $n = 30$  males) and right IOFC activity in individualists ( $n = 30$  males) encode social value distance relative to an individual-specific reference point. **a**, Coronal view of activations in the amygdala that encode the social value distance, the difference between potential and preferred self–other allocations, was significantly stronger in prosocials than individualists under placebo ( $P < 0.05$ , FWE-corrected at the cluster level after voxel-wise thresholding at  $P < 0.001$ ). **b**, Axial view of right IOFC activity encoding social value distance to a greater degree in individualists than prosocials (voxel-wise threshold  $P < 0.001$ , small volume correction  $P < 0.05$  for an anatomically defined right IOFC mask). Independent-samples  $t$ -tests were used in **a** and **b** on the beta estimates from ROIs of amygdala ( $t(58) = 2.75$ ,  $P = 0.008$ , 95% CI = 0.05, 0.33) and right IOFC ( $t(58) = -2.41$ ,  $P = 0.019$ , 95% CI =  $-0.30$ ,  $-0.03$ ). The amygdala and right IOFC ROIs employed anatomically defined masks (amygdala based on AAL bilateral anatomical mask, an anatomically defined right IOFC mask, using combined connectivity-based parcellations 8–11 covering right IOFC<sup>33</sup>). Error bars represented s.e.m. across participants in each group; \* $P < 0.05$  and \*\* $P < 0.01$ .**

with Context ( $F(1,64) = 1.33$ ,  $P = 0.254$ ), suggesting that the lack of a prosocial effect of oxytocin in prosocials was not due to a ceiling effect given their relative ‘self-centered’ social value preference in the competitive compared to non-competitive context. A similar ANOVA on individualists showed that oxytocin increased prosociality for individualists across both competitive and non-competitive contexts (Treatment: ( $F(1,57) = 8.56$ ,  $P = 0.005$ ,  $\eta^2 = 0.131$ ; Treatment  $\times$  Context:  $F(1,57) = 0.018$ ,  $P = 0.894$ ). Furthermore, the ANOVA on  $\varphi$  (Fig. 2a,d), with Social Disposition and Treatment as between-subjects factors and Context as a within-subjects factor, revealed the expected significant main effect of Context ( $F(1,121) = 145.92$ ,  $P = 1.59 \times 10^{-22}$ ,  $\eta^2 = 0.55$ ), with decreased prosociality in the competitive context. There was a significant Social Disposition  $\times$  Treatment interaction ( $F(1,121) = 5.28$ ,  $P = 0.023$ ,  $\eta^2 = 0.042$ ). Moreover, this interaction was not affected by contexts ( $F(1,121) = 0.697$ ,  $P = 0.406$ ), suggesting that the oxytocin effect on promoting prosociality was selective to individualists across different contexts.

#### Amygdala in prosocials represents a social value distance signal.

Based on the behavioral model, we looked for brain regions that encoded the social value distance between potential and preferred allocations. We created a parametric modulator for the social value distance<sup>29,30</sup>:  $1 - \cos(\theta(t) - \varphi)$ , on the basis of our social reference model, where  $\theta(t)$  is the angle of a current allocation at trial  $t$  and  $\varphi$  is the individual-specific reference point. This measure reflects the degree to which an allocation deviates from the reference point, with higher values indicating greater distance (that is, lower desirability) between potential and preferred allocations. At the second-level analysis, we found that the posterior cingulate cortex (peak coordinate in Montreal Neurological Institute (MNI) space:  $-6/-64/42$ ) and middle frontal gyrus (peak coordinate in MNI space:  $-34/8/54$ ) encoded social value distance when collapsing over the four groups (whole-brain significant at a voxel-wise threshold  $P < 0.001$  and a cluster-wise family-wise error (FWE) correction with  $P < 0.05$ ).

We then searched for brain regions that encoded the social value distance respectively for individualists and prosocials. We found that, under placebo, amygdala activity encoding social value distance was significantly stronger in prosocials than individualists (voxel-wise threshold  $P < 0.001$  and a cluster-wise FWE correction with  $P < 0.05$ , peak MNI coordinate:  $20/-10/-12$ , Fig. 3a and Supplementary Table 1). Previous studies have linked inhibition of

self-interest and top-down control of selfish behavior with right lateral prefrontal cortex<sup>17</sup>, such as right IOFC<sup>18,19</sup> and right dlPFC<sup>20</sup>. We hypothesized that individualists would represent deviation from preferred allocations mainly as a conflict with self-interest and a social value distance representation might be present in these areas. Comparison of individualists and prosocials under placebo revealed that right IOFC activity encoded social value distance to a greater degree in individualists than prosocials (voxel-wise threshold  $P < 0.001$ , small volume correction  $P < 0.05$  for an anatomically defined right IOFC mask, using combined connectivity-based parcellations 8–11 covering right IOFC<sup>33</sup>, Fig. 3b). This relationship was not present for right dlPFC. Further region of interest (ROI) analysis revealed a significant interaction between brain areas (right IOFC versus amygdala) and Social Disposition (individualists versus prosocials) under placebo ( $F(1, 58) = 11.63$ ,  $P = 0.0012$ ,  $\eta^2 = 0.167$ ). Here, the amygdala and right IOFC ROIs employed anatomically defined masks.

We extracted beta estimates associated with encoding social value distance from an anatomically defined amygdala ROI. We found that the strength of the amygdala social value distance representation was correlated with the degree of inequality aversion ( $r = 0.296$ ,  $P = 0.0012$ , Supplementary Fig. 7), whereas right IOFC activity bore no relationship to inequality aversion ( $r = -0.13$ ,  $P = 0.59$ ). A moderation analysis revealed that this positive correlation was stronger in prosocials than individualists ( $R^2$  change = 0.06,  $P = 0.003$ , Supplementary Fig. 7).

#### Oxytocin modulates social value representations in the amygdala in individualists.

We then searched for the main effect of Treatment and the interaction effect of Social Disposition and Treatment in the whole brain. There was no significant main effect of Treatment. The Social Disposition  $\times$  Treatment interaction  $F$  contrast revealed a significant cluster in the amygdala (Fig. 4a, peak voxels in the right amygdala survived voxel-wise FWE correction:  $P < 0.05$ ). Intranasal oxytocin selectively amplified the neural representation of social value distance in the amygdala of individualists, but not prosocials. A similar interaction pattern was found in other brain regions, including the right temporoparietal junction (TPJ) and ventral striatum (Supplementary Fig. 8). Moreover, as illustrated in Supplementary Fig. 9a–d, amygdala activity increased as a function of deviation from an individual-specific reference point in prosocials under placebo (slope estimate of the linear fit, 0.222;  $P = 0.001$ ) and

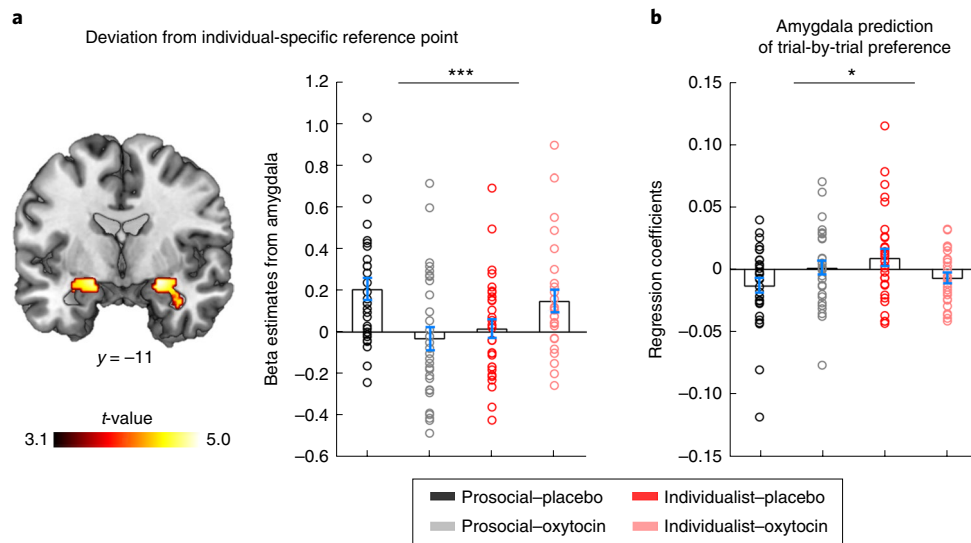


**Fig. 4 | Oxytocin promotes amygdala activity in representing social values in individualists ( $n_{\text{placebo}} = 30$ ,  $n_{\text{oxytocin}} = 26$  in individualists,  $n_{\text{placebo}} = 30$ ,  $n_{\text{oxytocin}} = 30$  in prosocials).** **a**, Coronal view of amygdala showing interaction effect between Treatment and Social Disposition (peak voxels in right amygdala, FWE-corrected  $P = 0.02$ ). Social Disposition-by-Treatment ANOVA showed significant interaction on the beta estimates from anatomically defined amygdala ( $F(1, 112) = 12.536$ ,  $P = 5.83 \times 10^{-4}$ ,  $\eta^2 = 0.101$ ). **b**, Trial-by-trial amygdala responses in predicting preference rating, after controlling for predicted social value distance for each trial. The Social Disposition-by-Treatment ANOVA on the trial-by-trial correlation coefficient showed a significant interaction between Social Disposition and Treatment ( $F(1, 112) = 6.722$ ,  $P = 0.011$ ,  $\eta^2 = 0.057$ ). Error bars represented s.e.m. across participants in each group, \* $P < 0.05$  and \*\*\* $P < 0.001$ .

this pattern was not found under oxytocin (slope estimate, 0.010;  $P = 0.88$ ). In contrast, amygdala activity increased as a function of deviation from an individual-specific referencepoint in individualists under oxytocin (slope estimate, 0.232;  $P = 0.003$ ) and this pattern was not found under placebo (slope estimate, 0.042;  $P = 0.50$ ). Amygdala responses were not related to absolute value differences or deviations from the allocentric reference (Supplementary Fig. 9e–l, all  $P > 0.5$ ).

We then examined the relationship between neural responses and evaluations of monetary allocations on a trial-by-trial basis to test whether the amygdala or right IOFC activity explained trial-by-trial variation in subjective preference ratings that was independent of the predicted social value distance. At the first-level (individual-subject-level) analysis, we modeled each trial separately and extracted beta estimates for amygdala and right IOFC for each trial. We then regressed the trial-by-trial amygdala and right IOFC responses (as  $x$  in the regression), respectively, onto the evaluation made for each monetary allocation on each trial (as  $y$  in the regression), while controlling for the deviation of each potential allocation from the individual-specific reference point. In doing so, we ensure that the beta estimates associated with the trial-by-trial amygdala and right IOFC activity reflect unique variance in predicting preference ratings based on amygdala and right IOFC responses above and beyond variance explained by predicted social value distance. We conducted a Social Disposition-by-Treatment ANOVA on the trial-by-trial correlation coefficient and found a significant interaction between Social Disposition and Treatment ( $F(1, 112) = 6.722$ ,  $P = 0.011$ ,  $\eta^2 = 0.057$ , Fig. 4b). The amygdala responses in prosocials negatively predicted trial-by-trial preference ratings under placebo, which was reduced by oxytocin. In contrast, amygdala activity negatively predicted trial-by-trial preference ratings in individualists under oxytocin versus placebo. The negative correlation indicated that the stronger the amygdala activity encoding social value distance, the lower the preference. This pattern of results was consistent with the amygdala providing an input signal for preferences, and fluctuations in the amygdala responses can explain trial-by-trial

deviations from average preferences. No such results were found for right IOFC activity.

Furthermore, we conducted a general linear model (GLM) with preference rating for each monetary allocation as a parametric modulator to identify any neural activity sensitive to subjective preference ratings. We found activity in the medial prefrontal cortex (mPFC) and IOFC, brain regions typically associated with value-coding<sup>34,35</sup>, correlated with subjective preference ratings for monetary allocations collapsing across the four groups. Moreover, there was a significant interaction between Social Disposition and Treatment for the mPFC and IOFC activity that encoded preference ratings (height threshold  $P < 0.001$ , cluster-based FWE correction,  $P < 0.05$ ; Supplementary Fig. 10). No significant Social Disposition  $\times$  Treatment interaction was found in the amygdala encoding the preference rating at the whole-brain or ROI level, suggesting that the amygdala activity encoding social value distance does not simply reflect the reverse of the preference signal.

We performed a generalized psycho-physiological interaction (gPPI) analysis with anatomically defined bilateral amygdala as the seed region at the whole-brain level. We found that amygdala activity encoding social value distance was coupled with ventral mPFC activity. Moreover, amygdala-vmPFC coupling was stronger in prosocials than in individualists under placebo (height threshold  $P < 0.001$ , uncorrected, Supplementary Fig. 11). Further, the ROI analysis suggested that oxytocin increased the strength of functional connectivity between amygdala and vmPFC in encoding social value distance in individualists (independent-samples  $t$ -test,  $t(54) = 2.69$ ,  $P = 0.009$ ) but not in prosocials ( $t(58) = 0.067$ ,  $P = 0.95$ , Supplementary Fig. 11). Given that the vmPFC is typically associated with value computation and value-guided choice<sup>34,35</sup>, these results may suggest a potential amygdala pathway linked to social preferences and social value-based decisions, which can be modulated by oxytocin in individualists.

## Discussion

Our results suggest that the representation of social values is a relational map that encodes the distance between potential values for

oneself and others on the same coordinate system. This representation can guide how we interact with others and how we respond to perceived unfairness. We provide empirical evidence that social value representations are constructed in relation to individual-specific social preferences, with the distance between potential and preferred allocations determining the value of social allocations. Prosocials represent social values relative to a more prosocial reference point than individualists, even in a competitive social context where self- and other-interest are in direct competition. Moreover, the social reference point derived from our social reference model accounts for individual variation in prosocial behaviors (for example, cooperation, generosity and inequality aversion) and therefore could serve as a compact description of social decision-making.

This dissimilarity distance measure bears some similarity to variables in value-based decision-making frameworks<sup>2</sup>. Social value distance is encoded by the amygdala in prosocials: the more dissimilar a potential allocation to the individual-specific reference point (that is, their preferred allocation), the greater the amygdala response. Our results offer a mechanistic account of how social value representations contribute to decision-making in prosocials. Trial-by-trial amygdala activity encoding social value distance reflects how attractive potential social allocations are judged to be by prosocials (that is, the stronger the amygdala response, the less attractive the allocation). Our control analyses show that amygdala activity is better explained by individual-specific reference points than by egocentric or allocentric frames of reference (Methods). Thus, amygdala activity might encode the difference between potential and preferred allocations (that is, a 'surprise' signal) much like dopamine firing represents reward prediction errors reflecting the difference between outcomes and expectations<sup>10</sup>.

We found an amygdala representation of social value distance that reflects a deviation from the most preferred allocation (what an individual hopes the allocation to be). This result is consistent with studies in both nonhuman primates<sup>7</sup> and in human neuroimaging studies<sup>16</sup> suggesting that the amygdala represents how undesirable an outcome is. Providing further support, we found that trial-by-trial amygdala activity was negatively correlated with the desirability of potential self–other allocations. Moreover, we found evidence that social value distance is also encoded by neural responses in the ventral striatum and TPJ in prosocials, consistent with previous findings linking prosocial decisions with several hubs in the social brain network<sup>7,36</sup>, including the amygdala, ventral striatum and TPJ. For example, TPJ activity encodes the subjective value of altruistic choice and the value of generosity<sup>36–38</sup>.

We also found evidence for a social value distance representation in the right IOFC in individualists relative to prosocials, which may reflect a distinct coding scheme for representing social values, although this activity did not survive whole-brain cluster-level correction and was not predictive of trial-by-trial preference ratings or modulated by oxytocin. However, this pattern is consistent with previous studies related to right IOFC function<sup>39</sup>. Right IOFC activation is associated with inhibition of self-interest, reward-guided decisions and detecting and evaluating threats to self-interest<sup>18,19</sup>. The right dlPFC, another region implicated in social decision-making and top-down control of selfish behavior<sup>20</sup>, did not have any significant social value distance representation in either individualists or prosocials.

Taken together, individuals may consider or calculate self-interest, altruistic values and evaluation of threat to self-interest when comparing potential and preferred allocations. These processes differ among individuals with different social orientations. Social value distance signals in prosocials may also relate to mentalizing about the needs of others<sup>36,37</sup>, integrating social information into estimates of subjective value<sup>40</sup> and calculating altruistic values<sup>41</sup> in the social brain network. However, it is possible that individualists perceive deviations from their preferred allocation mainly as conflicts with

self-interest, consistent with studies related to inhibition of self-interest conflict and evaluating threats to self-interest<sup>18,19</sup>.

Oxytocin is believed to facilitate social approach and to increase the salience of social cues in promoting adaptive social behaviors<sup>21</sup>. While individualists focus on self-interest and personal goals when making decisions<sup>3,4</sup>, oxytocin may increase prosociality by shifting reference points to more prosocial allocations and increasing the weights of outcomes for others, possibly through amplifying the amygdala representation of social value distance. This is consistent with studies showing that the amygdala plays a critical role in allocating attention to other people<sup>7</sup>, and in integrating social information<sup>42</sup> and social emotions<sup>13</sup> into decision-making. However, oxytocin fails to show a prosocial effect in prosocials. This does not necessarily mean that oxytocin makes prosocials greedy, as we found that prosocials still have greater prosociality than individualists under oxytocin. This is also not likely to be a ceiling effect, as there is no oxytocin effect on increasing prosociality even when prosocials employ a more self-centered reference point in a competitive context.

We found that oxytocin significantly reduces the strength of amygdala social value distance representations in prosocials and this was associated with a trend toward reduced prosociality. More sensitive changes in neural responses have often been observed in previous studies of prosocial behavior<sup>43</sup>. In the current study, one possible account is that social desirability or social pressure prevents prosocials from engaging in more self-centered performance. Although oxytocin significantly reduces amygdala representations of social values, consideration of both reputation<sup>44</sup> and others' approval<sup>45</sup> may prevent neural effects from translating into explicit changes in behavior. Finally, in the within-subjects oxytocin-replication experiment, we showed that the oxytocin effect on shifting the social reference point toward greater prosociality varied as a function of an individual's disposition of SVO, suggesting that the dichotomous comparison in the between-subjects design may prevent identification of an effect that depends on individual disposition.

Oxytocin has been implicated in many social behaviors, from promoting trust, generosity and cooperation<sup>21,22,46,47</sup> to aggravating mistrust and aggressive behavior<sup>48,49</sup>. The variable nature of oxytocin effects on prosociality is increasingly recognized. Seemingly contradictory oxytocin effects may be moderated by poorly understood individual and contextual differences<sup>21,24</sup>. Our finding of distinct oxytocin effects on the social reference point for prosocials and individualists provides evidence for the underlying computational and neural basis for oxytocin's effect on prosociality and helps reconcile conflicting results in the literature. A concern in previous studies is that post hoc explorations of different modulations by individual differences risk inflating the rate of Type I errors<sup>50</sup>. The current study examined only a single a priori specified modulator as we screened participants for social disposition before the oxytocin experiment, which allowed us to specifically test for different effects of oxytocin in prosocials and individualists. We consistently found across multiple studies that the selective effect of oxytocin on promoting prosociality in individualists was present in both competitive and non-competitive contexts, in both within- and between-subjects designs and with different experimental task designs.

Taken together, our results reveal a neural mechanism that underlies social value representations, providing new insights into the processes that influence human social decisions. Our results demonstrate that oxytocin adaptively modulates social value representations in the amygdala and indicate a fundamental role of oxytocin in social decision-making. These insights and the identification of a selective effect of oxytocin on prosociality in individualists may have implications for treating neuropsychiatric disorders with social deficits, including autism and sociopathy.

## Online content

Any methods, additional references, Nature Research reporting summaries, source data, statements of data availability and associated accession codes are available at <https://doi.org/10.1038/s41593-019-0351-1>.

Received: 16 January 2018; Accepted: 31 January 2019;  
Published online: 25 March 2019

## References

- Sanfey, A. G. Social decision-making: insights from game theory and neuroscience. *Science* **318**, 598–602 (2007).
- Rangel, A., Camerer, C. & Montague, P. R. A framework for studying the neurobiology of value-based decision making. *Nat. Rev. Neurosci.* **9**, 545–556 (2008).
- Haruno, M. & Frith, C. D. Activity in the amygdala elicited by unfair divisions predicts social value orientation. *Nat. Neurosci.* **13**, 160–161 (2010).
- Declerck, C. H., Boone, C. & Kiyonari, T. The effect of oxytocin on cooperation in a prisoner's dilemma depends on the social context and a person's social value orientation. *Soc. Cogn. Affect. Neurosci.* **9**, 802–809 (2014).
- Van Lange, P. A. M. The pursuit of joint outcomes and equality in outcomes: an integrative model of social value orientation. *J. Pers. Soc. Psychol.* **77**, 337–349 (1999).
- Chang, S. W. et al. Neuroethology of primate social behavior. *Proc. Natl Acad. Sci. USA* **110**, 10387–10394 (2013).
- Chang, S. W. et al. Neural mechanisms of social decision-making in the primate amygdala. *Proc. Natl Acad. Sci. USA* **112**, 16012–16017 (2015).
- Will, G.-J., Rutledge, R. B., Moutoussis, M. & Dolan, R. J. Neural and computational processes underlying dynamic changes in self-esteem. *eLife* **6**, 6 (2017).
- Gottfried, J. A., O'Doherty, J. & Dolan, R. J. Encoding predictive reward value in human amygdala and orbitofrontal cortex. *Science* **301**, 1104–1107 (2003).
- Schultz, W., Dayan, P. & Montague, P. R. A neural substrate of prediction and reward. *Science* **275**, 1593–1599 (1997).
- Boccia, M. L., Petrusz, P., Suzuki, K., Marson, L. & Pedersen, C. A. Immunohistochemical localization of oxytocin receptors in human brain. *Neurosci.* **253**, 155–164 (2013).
- Haber, S. N. & Knutson, B. The reward circuit: linking primate anatomy and human imaging. *Neuropsychopharmacology* **35**, 4–26 (2010).
- Bickart, K. C., Dickerson, B. C. & Barrett, L. F. The amygdala as a hub in brain networks that support social life. *Neuropsychologia* **63**, 235–248 (2014).
- Paton, J. J., Belova, M. A., Morrison, S. E. & Salzman, C. D. The primate amygdala represents the positive and negative value of visual stimuli during learning. *Nature* **439**, 865–870 (2006).
- De Martino, B., Camerer, C. F. & Adolphs, R. Amygdala damage eliminates monetary loss aversion. *Proc. Natl Acad. Sci. USA* **107**, 3788–3792 (2010).
- Garrett, N., Lazzaro, S. C., Ariely, D. & Sharot, T. The brain adapts to dishonesty. *Nat. Neurosci.* **19**, 1727–1732 (2016).
- Knock, D. & Fehr, E. Resisting the power of temptations: the right prefrontal cortex and self-control. *Ann. NY Acad. Sci.* **1104**, 123–134 (2007).
- Spitzer, M., Fischbacher, U., Herrnberger, B., Grön, G. & Fehr, E. The neural signature of social norm compliance. *Neuron* **56**, 185–196 (2007).
- Rudebeck, P. H., Saunders, R. C., Prescott, A. T., Chau, L. S. & Murray, E. A. Prefrontal mechanisms of behavioral flexibility, emotion regulation and value updating. *Nat. Neurosci.* **16**, 1140–1145 (2013).
- Haruno, M., Kimura, M. & Frith, C. D. Activity in the nucleus accumbens and amygdala underlies individual differences in prosocial and individualistic economic choices. *J. Cogn. Neurosci.* **26**, 1861–1870 (2014).
- Ma, Y., Shamay-Tsoory, S., Han, S. & Zink, C. F. Oxytocin and social adaptation: Insights from neuroimaging studies of healthy and clinical populations. *Trends Cogn. Sci.* **20**, 133–145 (2016).
- Zink, C. F. & Meyer-Lindenberg, A. Human neuroimaging of oxytocin and vasopressin in social cognition. *Horm. Behav.* **61**, 400–409 (2012).
- Alvares, G. A., Hickie, I. B. & Guastella, A. J. Acute effects of intranasal oxytocin on subjective and behavioral responses to social rejection. *Exp. Clin. Psychopharmacol.* **18**, 316–321 (2010).
- Ma, Y., Liu, Y., Rand, D. G., Heatherton, T. F. & Han, S. Opposing oxytocin effects on intergroup cooperative behavior in intuitive and reflective minds. *Neuropsychopharmacology* **40**, 2379–2387 (2015).
- Scheele, D. et al. Oxytocin modulates social distance between males and females. *J. Neurosci.* **32**, 16074–16079 (2012).
- Chang, S. W., Barter, J. W., Ebitz, R. B., Watson, K. K. & Platt, M. L. Inhaled oxytocin amplifies both vicarious reinforcement and self reinforcement in rhesus macaques (*Macaca mulatta*). *Proc. Natl Acad. Sci. USA* **109**, 959–964 (2012).
- Lambert, B., Declerck, C. H., Boone, C. & Parizel, P. M. A functional MRI study on how oxytocin affects decision making in social dilemmas: Cooperate as long as it pays off, aggress only when you think you can win. *Horm. Behav.* **94**, 145–152 (2017).
- Murphy, R. O., Ackermann, K. A. & Handgraaf, M. Measuring social value orientation. *Judgm. Decis. Mak.* **6**, 771–781 (2011).
- Constantinescu, A. O., O'Reilly, J. X. & Behrens, T. E. J. Organizing conceptual knowledge in humans with a gridlike code. *Science* **352**, 1464–1468 (2016).
- Doeller, C. F., Barry, C. & Burgess, N. Evidence for grid cells in a human memory network. *Nature* **463**, 657–661 (2010).
- Evans, A. M. & Rand, D. G. Cooperation and decision time. *Curr. Opin. Psychol.* **26**, 67–71 (2018).
- Krajbich, I., Bartling, B., Hare, T. & Fehr, E. Rethinking fast and slow based on a critique of reaction-time reverse inference. *Nat. Commun.* **6**, 7455 (2015).
- Neubert, F. X., Mars, R. B., Thomas, A. G., Sallet, J. & Rushworth, M. F. Comparison of human ventral frontal cortex areas for cognitive control and language with areas in monkey frontal cortex. *Neuron* **81**, 700–713 (2014).
- Lim, S. L., O'Doherty, J. P. & Rangel, A. The decision value computations in the vmPFC and striatum use a relative value code that is guided by visual attention. *J. Neurosci.* **31**, 13214–13223 (2011).
- Jocham, G., Hunt, L. T., Near, J. & Behrens, T. E. A mechanism for value-guided choice based on the excitation-inhibition balance in prefrontal cortex. *Nat. Neurosci.* **15**, 960–961 (2012).
- Morishima, Y., Schunk, D., Bruhin, A., Ruff, C. C. & Fehr, E. Linking brain structure and activation in temporoparietal junction to explain the neurobiology of human altruism. *Neuron* **75**, 73–79 (2012).
- Hutcherson, C. A., Bushong, B. & Rangel, A. A neurocomputational model of altruistic choice and its implications. *Neuron* **87**, 451–462 (2015).
- Strombach, T. et al. Social discounting involves modulation of neural value signals by temporoparietal junction. *Proc. Natl Acad. Sci. USA* **112**, 1619–1624 (2015).
- Kringelbach, M. L. The human orbitofrontal cortex: linking reward to hedonic experience. *Nat. Rev. Neurosci.* **6**, 691–702 (2005).
- Ruff, C. C. & Fehr, E. The neurobiology of rewards and values in social decision making. *Nat. Rev. Neurosci.* **15**, 549–562 (2014).
- Telzer, E. H., Fuligni, A. J., Lieberman, M. D. & Galván, A. Neural sensitivity to eudaimonic and hedonic rewards differentially predict adolescent depressive symptoms over time. *Proc. Natl Acad. Sci. USA* **111**, 6600–6605 (2014).
- Mosher, C. P., Zimmerman, P. E. & Gothard, K. M. Neurons in the monkey amygdala detect eye contact during naturalistic social interactions. *Curr. Biol.* **24**, 2459–2464 (2014).
- Hein, G., Morishima, Y., Leiberg, S., Sul, S. & Fehr, E. The brain's functional network architecture reveals human motives. *Science* **351**, 1074–1078 (2016).
- Ariely, D., Bracha, A. & Meier, S. Doing good or doing well? Image motivation and monetary incentives in behaving prosocially. *Am. Econ. Rev.* **99**, 544–555 (2009).
- Bénabou, R. & Tirole, J. Incentives and prosocial behavior. *Am. Econ. Rev.* **96**, 1652–1678 (2006).
- Aydogan, G. et al. Oxytocin promotes altruistic punishment. *Soc. Cogn. Affect. Neurosci.* **12**, 1740–1747 (2017).
- Yan, X., Yong, X., Huang, W. & Ma, Y. Placebo treatment facilitates social trust and approach behavior. *Proc. Natl Acad. Sci. USA* **115**, 5732–5737 (2018).
- Neeman, R., Perach-Barzilay, N., Fischer-Shofty, M., Atias, A. & Shamay-Tsoory, S. G. Intranasal administration of oxytocin increases human aggressive behavior. *Horm. Behav.* **80**, 125–131 (2016).
- Radke, S. & de Bruijn, E. R. The other side of the coin: oxytocin decreases the adherence to fairness norms. *Front. Hum. Neurosci.* **6**, 193 (2012).
- Nave, G., Camerer, C. & McCullough, M. Does oxytocin increase trust in humans? A critical review of research. *Perspect. Psychol. Sci.* **10**, 772–789 (2015).

## Acknowledgements

We thank H. Zhang, D. Wang, X. Zou and H. Wang for their assistance in data collection. This work was supported by the National Natural Science Foundation of China (Project nos. 31722026, 91632118, 31771204 and 31661143039 to Y.M.), the Fundamental Research Funds for the Central Universities (grant nos. 2017XTCX04 and 2018EYT04 to Y.M.), the Open Research Fund of the State Key Laboratory of Cognitive Neuroscience, Beijing Normal University (to Y.M.), startup funding from the State Key Laboratory of Cognitive Neuroscience and Learning, the IDG/McGovern Institute for Brain Research, Beijing Normal University (to Y.M.), by the International Max Planck Research School on Computational Methods in Psychiatry and Ageing Research (IMPRS COMP2PSYCH



to Y.L.), and by the Max Planck Society and a MRC Career Development Award (no. MR/N02401X/1 to R.B.R.)

### Author contributions

Y.M. conceived and designed the project and designed the fMRI experiment. Y.M. and Y.L. designed the replication experiments. W.Li., X.W., X.P. and Y.M. performed the fMRI experiment. S.L. and X.Y. performed the replication experiments. Y.L., S.L., W.Lin. and Y.M. analyzed the data and interpreted the results of the fMRI and behavioral experiments. Y.L., W.Lin., R.B.R. and Y.M. wrote the paper.

### Competing interests

The authors declare no competing interests.

### Additional information

**Supplementary information** is available for this paper at <https://doi.org/10.1038/s41593-019-0351-1>.

**Reprints and permissions information** is available at [www.nature.com/reprints](http://www.nature.com/reprints).

**Correspondence and requests for materials** should be addressed to Y.M.

**Journal peer review information:** *Nature Neuroscience* thanks Bruno Averbeck, Andreas Meyer-Lindenberg, and the other anonymous reviewer(s) for their contribution to the peer review of this work.

**Publisher's note:** Springer Nature remains neutral with regard to jurisdictional claims in published maps and institutional affiliations.

© The Author(s), under exclusive licence to Springer Nature America, Inc. 2019

## Methods

**Participants.** For the oxytocin-fMRI and behavioral oxytocin-replication experiments, we recruited only male participants to avoid potential confounds of sex differences in oxytocin effects<sup>21,51</sup>, consistent with previous studies examining oxytocin effects on social cognition<sup>52,53</sup>. All participants had normal or corrected-to-normal vision and reported no history of neurological or psychiatric diagnoses, or medication, drug or alcohol abuse. Participants provided informed consent after the experimental procedure had been fully explained and were informed of their right to withdraw at any time during the study. The experimental protocol was in line with the standards of the Declaration of Helsinki and approved by the research ethics committee at the State Key Laboratory of Cognitive Neuroscience and Learning, Beijing Normal University (Beijing, China).

**Oxytocin-fMRI experiment.** There were 282 male college students (mean age =  $22.3 \pm 2.12$  years) that participated in this study as paid volunteers. Each participant's disposition in SVO was measured in the behavioral session (149 prosocials and 83 individualists were identified). Among these, 127 participants were qualified and willing to participate in the fMRI experiment (at least 7 days after the behavioral session). Two participants (1.6%) were excluded due to technical issues during scanning, leaving 125 participants in the behavioral analysis (individualists under placebo:  $n = 30$  males, mean age  $22.2 \pm 2.35$  years, under oxytocin:  $n = 29$  males, mean age  $21.7 \pm 2.39$  years; prosocials under placebo:  $n = 31$  males, mean age  $22.1 \pm 2.70$  years, under oxytocin:  $n = 35$  males, mean age  $22.1 \pm 2.70$  years). An additional nine participants (7.2%) were excluded from further fMRI analysis due to excessive head movement during scanning ( $>3$  mm), leaving 116 participants for fMRI data analysis. In the end, there were 60 prosocials including 30 administered placebo (mean age,  $22.7 \pm 2.61$  years) and 30 administered oxytocin (mean age,  $21.8 \pm 2.38$  years), and 56 individualists including 30 administered placebo (mean age,  $23.0 \pm 2.29$  years) and 26 administered oxytocin (mean age,  $22.5 \pm 3.03$  years) in the formal fMRI data analysis. Prosocials and individualists receiving oxytocin or placebo were matched on state and trait anxiety, depression, subjective well-being and happiness ratings (all  $P > 0.05$  on both the main and interaction effects of Treatment and Social Disposition, Supplementary Table 3).

The sample size of the fMRI study was determined before data collection. We conducted sample size estimation using G\*Power v.3.1 (ref. <sup>54</sup>) to determine the number of participants sufficient to detect a reliable effect. Based on an estimated average small-to-medium effect size of oxytocin effect on social behaviors (Cohen's  $d = 0.28$ )<sup>55</sup>, 104 participants were needed to detect a significant effect ( $\alpha = 0.05$ ,  $\beta = 0.80$ , two-by-two mixed ANOVA interaction effects). We planned to recruit 125 participants (assuming 10–20% participants would be removed from the fMRI data analysis due to excessive head movement). In the end, we recruited 127 participants because the 41th and 42th participants did not complete the experiment due to technical issues during scanning. For comparison, we also considered the 58 oxytocin-fMRI studies published at the time we initiated our experiment in June 2015, of which 23 employed between-subject design recruiting healthy individuals<sup>56</sup>. On average, the sample size was 50.89 in total, 25.82 for the placebo group and 25.47 for the oxytocin group. Thus, our planned sample size of 125 participants was a decent sample size compared to the average across oxytocin-fMRI studies. Moreover, the sample size of 116 participants (after removal of subjects due to technical issues and excessive head movement) was adequate to reveal reliable effects, exceeding the 104 participants needed for 80% power.

**Oxytocin-replication experiment.** We conducted an additional behavioral experiment for the replication of the oxytocin effect using a double-blind, randomized, placebo-controlled, within-subjects crossover design. The sample size was predetermined on the basis of the effect size (Cohen's  $d = 0.45$ ) from our original finding in the fMRI study. The G\*Power calculation suggested that 40 participants (20 for each group) were required to detect a reliable effect ( $\alpha = 0.05$ ,  $\beta = 0.80$  for a within (oxytocin versus placebo)-between (prosocial versus individualist) interaction). To obtain a better sense of the robustness of the original findings, we doubled the estimated sample size, aiming to enroll 40 participants per group, with corresponding power equal to 98%. We replicated the selective oxytocin effects on promoting prosociality (that is,  $\phi$ ) in individualists in the whole sample (40 prosocials and 40 individualists), as well as in the first 20 prosocials and 20 individualists (as estimated by the G\*Power analysis). A total of 140 males (mean age,  $22.33 \pm 3.35$  years) were invited to a behavioral session to identify their disposition in SVO. Among these, 82 participants were qualified and willing to participate in the oxytocin experiment (at least 7 days after the first behavioral session). Two participants did not show up for the second session. Thus, 80 participants (40 prosocials, mean age,  $22.08 \pm 3.47$  years; 40 individualists; mean age,  $21.54 \pm 2.42$  years) were included in the final data analysis.

**Online-replication experiment.** We conducted an online experiment with a large sample ( $n = 315$ , 132 males, 160 prosocials, mean age =  $22.40 \pm 3.27$ ; 155 individualists, mean age =  $22.48 \pm 3.30$ ) to provide a replication for our finding that the social reference model outperforms other models. Prosocials and individualists did not differ in their ratings on the first impression, likeability and attractiveness of the online partner (independent-samples  $t$ -test, impression:  $t(313)$

= 1.03,  $P = 0.305$ ; likeability:  $t(313) = 0.98$ ,  $P = 0.328$ ; attractiveness:  $t(313) = 0.73$ ,  $P = 0.465$ ).

**Procedure.** Participants were first invited to the behavioral session to identify their social disposition and be screened for eligibility of the fMRI and oxytocin behavioral experiments. Participants recruited in the fMRI experiment were randomly assigned to the intranasal administration of oxytocin or placebo in a double-blind placebo-controlled between-subjects design. In the oxytocin experiment, participants received either oxytocin or placebo intranasally in two separate sessions, with a 5–7-day washout period between two sessions. The order of oxytocin and placebo treatment was counterbalanced across participants. All participants were instructed to abstain from cigarette, alcohol and caffeine during the 24 h before the experiment, and to refrain from eating or drinking anything except water for 2 h before the experiment. Participants self-administered oxytocin or placebo 35 min (ref. <sup>57</sup>) before the main task; that is, a monetary outcome-pair evaluation task (a revised one with monetary pairs sampled on three circles of different circumference was used in the oxytocin-replication experiment).

**Social disposition measurements.** In the fMRI and the oxytocin-replication experiments, participants were first invited to a behavioral session to identify their dispositions in social preference. In the behavioral session, all participants provided demographic information and completed the triple dominance<sup>5</sup> and SVO<sup>28</sup> tasks, which were conventional measurements of one's stable disposition in SVO. To incentivize authentic responses during social interactions, participants were recruited in groups of 8–10 individuals (all were strangers to each other). For each economic game, participants were paired with a new, mutually anonymous partner.

The triple dominance task is a nine-item measure of one's social disposition by asking participants to choose from three types of hypothetical self-other monetary allocation option (for example, prosocial option: self = 100, other = 100; individualistic option: self = 110, other = 60 and competitive option: self = 100, other = 20). Based on their decisions to the nine items, participants were classified as prosocial (who chose prosocial options on six or more items), individualist (who chose individualistic options on six or more items) or competitor (who chose competitive responses on six or more items). Participants who failed to choose the same type of options on at least six items were referred to as 'unidentified'. In the current study, we referred to both 'individualist' and 'competitor' as 'individualists' in comparison to 'prosocial'.

The SVO slider measure included six primary items and nine secondary items. For each item, participants were asked to choose the most preferred one from nine monetary allocation choices over a well-defined continuum of joint payoffs. Based on the inverse tangent of the ratio between mean allocations for the self and the paired partner, the six primary items yielded a measure that categorized participants into: altruist, prosocial, individualist and competitor<sup>28</sup>. Here, we referred to both 'altruist' and 'prosocial' as prosocials (that is,  $SVO^\circ > 22.45^\circ$ ), and both individualist and competitor as individualists (that is,  $SVO < 22.45^\circ$ ). The scores of nine secondary items of SVO are used to calculate an independent measure of inequality aversion; that is, the general preference for fairness and resistance to inequalities. To ensure a reliable measure of social disposition, only participants who were consistently classified by the triple dominance and SVO tasks were deemed qualified (either prosocial or individualist).

**Prosocial behavior measures.** Participants were also invited to the public goods game and the dictator game. The contribution participants made in these two games have been separately used as indicators of the levels of cooperation and altruism—two key characteristics of prosocial behaviors<sup>24,58–60</sup>.

In the four-player public goods game, participants initially received 80 experimental monetary units and decided the amount of monetary units to contribute to a four-player common project versus to keep for themselves. The money contributed to the common project would be doubled and evenly divided among the four players. The final payoff was equal to the sum of money they kept for the self and money split from the common project. The amount of money contributed to the common project reflected cooperative behavior.

In the dictator game, 'the dictator' (that is, the participant), determined how to split 80 monetary units between himself and another player. The other players, 'the recipient', simply received the remainder of the endowment left by the dictator. The recipient's role was entirely passive and had no input into the outcome of the game. The amount the dictator sent to the recipient indicated his altruistic behavior.

**fMRI session.** A pair of participants, who were strangers to each other, was invited to the fMRI experiment at the same time. On arrival, participants' moods were measured using the Positive and Negative Affect Scale, which was later measured again after the experiment to quantify potential mood change. There was no significant mood change overall and no significant interaction effect with division of Social Disposition or Treatment (Supplementary Table 4). We measured participants' salivary oxytocin baseline levels by collecting their salivary samples before oxytocin or placebo administration (Supplementary Fig. 4). There was no significant main effect or interaction effect between Social Disposition and Treatment on the salivary oxytocin level. Each pair of participants was given 5 min

to introduce themselves to each other to strengthen the oxytocin effect on social cognition<sup>61</sup>. We ensured that participants introduced their names to each other, which were also presented on the screen for each monetary allocation. Participants in each pair were scanned in sequence and randomly treated with oxytocin or placebo. The procedure of oxytocin or placebo administration was similar to previous research<sup>24</sup>. A single dose of 24 international units (IU) of oxytocin or placebo (containing the active ingredients except for the neuropeptide) was intranasally self-administered by nasal spray approximately 35 min before the fMRI scanning under an experimenter's supervision. The spray was administered to participants three times with each administration consisted of one inhalation of 4 IU into each nostril. The choice of 24 IU oxytocin and its effect on brain oxytocin level is explained in Supplementary Note 1. After scanning, participants were asked to perform a similar post-scan monetary outcome-pair evaluation task in a competitive context. The duration of the fMRI scanning and the post-scan test were carefully controlled within the time frame of the oxytocin peak response in the brain<sup>57</sup>.

**Monetary outcome-pair evaluation task during MRI scanning.** In the MRI scanner, participants were presented with pairs of monetary outcomes assigned to the self and the paired participant (referred to as the partner). Participants evaluated their preference of each monetary allocation on a four-point Likert scale (1 = least preferable to 4 = most preferable) by a button press. To encourage genuine responses and minimize the influences of social norms or social pressure, the preference ratings were unknown to the other player. Participants were told that their preference rating for each monetary outcome pair would determine the overall gains for self ( $G_s$ ) and the partner ( $G_p$ ), that is,  $G_s = \sum m_i \times p_i$ , and  $G_p = \sum m_p \times p_p$ , where  $p_i$  is participant's preference rating for the monetary outcome pair,  $i$ ;  $m_i/m_p$  is the monetary amount for self or the partner in monetary pair,  $i$ . In each trial, the monetary allocation was presented for 3 s, followed by a jittered time interval, pseudo-randomized from 1 s to 5 s (with mean interval of 3 s; Fig. 1a). There were two sessions with 90 trials per session, presented in a random order.

To determine appropriate monetary allocations for the fMRI scanning, we first conducted a pilot behavioral experiment on an independent sample ( $n = 60$ ), where we included the full space of monetary outcome pairs and asked participants to rate their preference for each allocation on a nine-point Likert scale (1 = least preferable; 9 = most preferable). We found that participants reported invariably with the least preferable for pairs in the third quadrants and along the negative  $x$  or  $y$  axis, where both self and the partner lose money (average preference rating of 1.8 on a 1–9 scale, with no rating scores higher than 3). Therefore, these pairs (that is,  $\$Self \leq 0$  and/or  $\$Other \leq 0$ ) were not included in the fMRI task. The monetary outcome pairs for self and the partner, as illustrated in Fig. 1a, were designed in a way as to form angles that evenly sampled from  $-90^\circ$  to  $180^\circ$  with an interval approximately  $5^\circ$ , based on an egocentric reference point (that is,  $0^\circ$ , which indicates perfect alignment with the positive  $x$  axis). We also included pairs where only the self or the partner gained money (evenly sampled along the positive  $x/y$  axis) while the opponent received zero. These pairs were used to generate functional masks for fMRI ROI analysis and were not included in formal behavioral analyses.

**Monetary outcome-pair evaluation task in a competitive context.** Participants completed a post-scan behavioral experiment largely the same as that in the fMRI task, but with two key differences. First, participants reported their preference of each monetary outcome pair on ten instead of four levels (0 = least preferable to 9 = most preferable). Second, we induced a self-interest and other-interest conflict situation by framing the payoff in a competitive context, where participants would get a bonus reward if and only if the sum of gains to the themselves was larger than that to the partner. Otherwise, they gained nothing (that is, winner takes all). Therefore, the self and partner's interest were in direct competition in this context. There was one session with 90 trials presented in a random order.

**Monetary outcome-pair evaluation task in oxytocin-replication and online-replication experiments.** The task design for the replication experiments was identical to the fMRI experiment except that the monetary pairs were sampled on three circles of different circumference (radius, 5, 6, 9), with  $\theta$  ranging from  $-90^\circ$  to  $180^\circ$  with different intervals ( $5^\circ$ ,  $17^\circ$ ,  $23^\circ$ ). There was one session with 82 trials presented in a random order.

**Behavioral analysis.** We constructed eight behavioral models based on theoretical considerations (Supplementary Fig. 2). For the social reference model (the winning model, Supplementary Fig. 2), we modeled  $z$ -scored preference ratings ( $P_i$ ) for each participant:  $P_i = \beta_1 \times \cos(\theta) + \beta_2 \times \sin(\theta)$ . In this model,  $\beta_1$  and  $\beta_2$  are weights for how much people care about the value of a potential payoff for themselves ( $\$Self$ ) and for the partner ( $\$Other$ ), respectively. The angle  $\theta$  depends on the difference between those values. We then computed a single individual-specific reference point  $\varphi$  for each participant on the basis of the ratio of  $\beta_1$  and  $\beta_2$ :  $\varphi = \arctan(\beta_2/\beta_1)$  (refs. 29,30; Fig. 1c). The social value distance reflects the difference between a potential self-other allocation  $\theta$  and a preferred allocation  $\varphi$  that reflects an individual-specific reference point against which potential allocations are compared.

When all monetary pairs lie on the circumference of a circle,  $\cos(\theta)$  can be seen simply as the amount offered to the self and  $\sin(\theta)$  as the amount offered to the other, divided by the radius of the circle. However, when including monetary pairs from circles with different radii (that is, the modified design used in additional experiments),  $\cos(\theta)$  and  $\sin(\theta)$  provide a compact index that permits investigation of the relationship between self and other in a value-insensitive way (since  $\cos(\theta)^2 + \sin(\theta)^2 = 1$ ).

**fMRI acquisition and preprocessing.** *Imaging acquisition.* Whole-brain imaging data was collected on a GE 3-Tesla magnetic resonance scanner with a standard head coil (HDx, Signa MR 750 System; GE Healthcare). Functional images were collected using an echo-planar imaging sequence (axial slices, 32; slice thickness, 4 mm; gap, 1 mm; repetition time, 2,000 ms; echo time, 30 ms; voxel size,  $3.75 \times 3.75 \times 5$  mm<sup>3</sup>; flip angle,  $90^\circ$ ; field of view  $240 \times 240$  mm<sup>2</sup> and 285 volumes for each session, two sessions in total). Structural images were acquired through three-dimensional sagittal T1-weighted magnetization-prepared rapid gradient echo (180 slices; repetition time, 8,208 ms; echo time, 3.22 ms; slice thickness, 1 mm; voxel size,  $0.47 \times 0.47 \times 1.0$  mm<sup>3</sup>; flip angle,  $12^\circ$ ; inversion time, 450 ms; field of view,  $240 \times 240$  mm<sup>2</sup>).

*Imaging preprocessing.* Brain imaging data was preprocessed using Statistical Parametric Mapping (SPM12; <http://www.fil.ion.ucl.ac.uk/spm>). The first five functional images from each session were discarded for signal equilibrium and participants' adaptation to scanning noise. Remaining images were corrected for slice acquisition timing and realigned for head motion correction. Subsequently, functional images were coregistered to each participant's gray matter image segmented from corresponding high-resolution T1-weighted image, then spatially normalized into a common stereotaxic MNI space and resampled into 2-mm isotropic voxels. Finally, images were smoothed by an isotropic three-dimensional Gaussian kernel with 8-mm full-width at half-maximum.

*GLM analysis.* After preprocessing, we estimated parameters of different GLMs. All models included regressors for monetary outcome pair presentation separately for trials on and off the  $x/y$  axis, button press, instructions, six nuisance regressors for motion-related artefacts and various parametric modulations associated with these regressors (detailed below). Parametric regressors were not orthogonalized in the design matrix, ensuring that parameter estimates were not confounded by spurious correlations due to signals related to other regressors<sup>62</sup>. All regressors (parametrically modulated or not) were convolved with the canonical hemodynamic response function in SPM before entering the GLM. Data were high-pass filtered at 1/128 Hz. We controlled for decision times for all fMRI analyses.

We created parametric regressors that were associated with the value distance or value difference between self and other, at the monetary outcome-pair presentation to search for brain regions that encoded the subjective distance in social value representation. In the fMRI analysis, we included ten GLM models: a social value distance from an individual-specific reference point (that is,  $1 - \cos(\theta(t) - \varphi)$ ,  $\theta(t)$  is the angle of a potential allocation at trial  $t$  and  $\varphi$  is the individual-specific reference point derived from our social reference model), an egocentric reference (that is,  $\cos(\theta(t))$ ), an allocentric reference (that is,  $\sin(\theta(t))$ ), an objective equality reference point (that is,  $\cos(\theta(t) - 45^\circ)$ ), monetary outcome for the self (that is,  $\$Self$ ), monetary outcome for the partner (that is,  $\$Other$ ), absolute value difference ( $|\$Self - \$Other|$ ) or advantageous (that is,  $\max(0, \$Self - \$Other)$ ) or disadvantageous inequality aversion (that is,  $\max(0, \$Other - \$Self)$ ) separately, or with preference rating as parametric modulator in the GLM.

In building different GLMs, we are not arguing that the social reference model is superior to other models in all environments nor claiming the dissimilarity measure is the best measure for capturing amygdala responses as this was not our aim<sup>63</sup>. Rather, we aimed to identify brain regions that could specifically represent deviations from the reference point of social preference.

Coefficients for each regressor were estimated for each participant using maximum likelihood estimates to account for serial correlations in the data. Statistical significance was determined at the group level using a random-effects analysis. Significant clusters from second-level analyses were determined using a height threshold of  $P < 0.001$  and an extent threshold of  $P < 0.05$  with cluster-based FWE correction. We also applied voxel-wise inference using the FWE-corrected threshold of  $P = 0.05$  on the whole-brain analysis, given recent concern over cluster-wise inferences. For the relationship between value distance ( $1 - \cos(\theta(t) - \varphi)$ ) and neural responses during monetary outcome-pair presentation, the peak voxels in right amygdala survived voxel-wise FWE correction ( $P = 0.02$ ).

*Control analysis of amygdala responses.* One alternative hypothesis of the amygdala activity pattern is that it encoded  $\$Other$  or  $\$Disadvantageous$  Inequality, instead of the dissimilarity distance to the reference point in our winning model, we reran the fMRI analysis from the first level controlling for  $\$Other$  and  $\$Disadvantageous$  Inequality as regressors in the GLM (without orthogonalization between regressors). We looked for the unique variance that can be explained by the dissimilarity distance to social reference point over and beyond the variance explained by  $\$Other$  or  $\$Disadvantageous$  Inequality. The main result of a

significant Social Disposition  $\times$  Treatment interaction on the amygdala activity in coding deviations from the social reference point was unchanged.

We further tested another possibility of the amygdala response: it encoded \$Other in proportion to its importance to the individual. To test this possibility, we built another GLM model with the parametric regressor,  $\beta_2 \times \$Other$ , where  $\beta_2$  represented the estimated weight of \$Other on social preference, reflecting the individual-specific importance of \$Other in social preference evaluation for each participant. However, the amygdala activity did not simply encode \$Other to the extent that it predicts social preferences, at the whole-brain level (height  $P < 0.001$ , cluster-wise FWE,  $P < 0.05$ ) or ROI (anatomically defined) level.

**Statistics.** The oxytocin-fMRI and oxytocin-replication experiments were double-blind; that is, both participants and experimenters were blind to experimental conditions (both treatment and social disposition conditions). Data analysis was not performed blind to the conditions of the experiments. We first conducted one-way ANOVA with Social Disposition as a between-subjects factor to compare the social reference point between individualists and prosocials under placebo. To evaluate the oxytocin effect on the social value representation, we conducted ANOVAs on behavioral and fMRI data, with Social Disposition (prosocial versus individualistic) and Treatment (oxytocin versus placebo) as between-subjects factors, followed by planned two-tailed  $t$ -tests to examine oxytocin effect separately in individualists and prosocials (independent-samples  $t$ -test for fMRI study and paired-samples  $t$ -test for the oxytocin-replication study). Data distribution was assumed to be normal but this was not formally tested. All correlations were performed by Pearson's correlation coefficient analysis.

**Reporting Summary.** Further information on research design is available in the Nature Research Reporting Summary linked to this article.

### Code availability

Analysis code to model the social value representation based on preference rating data is provided in the Supplementary Software.

### Data availability

The data that support the findings of this study and the analysis code are available from the corresponding author upon reasonable request.

## References

- Gao, S. et al. Oxytocin, the peptide that bonds the sexes also divides them. *Proc. Natl Acad. Sci. USA* **113**, 7650–7654 (2016).
- Zhang, H., Gross, J., De Dreu, C. & Ma, Y. Oxytocin promotes coordinated out-group attack during intergroup conflict in humans. *eLife*, **8**, e40698 (2019).
- Ma, Y., Li, S., Wang, C., Liu, Y., Li, W., Yan, X., Chen, Q. & Han, S. Distinct oxytocin effects on belief updating in response to desirable and undesirable feedback. *Proc. Natl Acad. Sci. USA*, **113**, 9256–9261 (2016).
- Faul, F., Erdfelder, E., Buchner, A. & Lang, A.-G. Statistical power analyses using G\*Power 3.1: tests for correlation and regression analyses. *Behav. Res. Method* **41**, 1149–1160 (2009).
- Walum, H., Waldman, I. D. & Young, L. J. Statistical and methodological considerations for the interpretation of intranasal oxytocin studies. *Biol. Psychiatry* **79**, 251–257 (2016).
- Wang, D., Yan, X., Li, M. & Ma, Y. Neural substrates underlying the effects of oxytocin: a quantitative meta-analysis of pharmaco-imaging studies. *Soc. Cogn. Affect. Neurosci.* **12**, 1565–1573 (2017).
- Paloyelis, Y. et al. A spatiotemporal profile of in vivo cerebral blood flow changes following intranasal oxytocin in Humans. *Biol. Psychiatry* **79**, 693–705 (2016).
- Rand, D. G., Greene, J. D. & Nowak, M. A. Spontaneous giving and calculated greed. *Nature* **489**, 427–430 (2012).
- Fehr, E. & Fischbacher, U. The nature of human altruism. *Nature* **425**, 785–791 (2003).
- Harbaugh, W. T., Mayr, U. & Burghart, D. R. Neural responses to taxation and voluntary giving reveal motives for charitable donations. *Science* **316**, 1622–1625 (2007).
- Declerck, C. H., Boone, C. & Kiyonari, T. Oxytocin and cooperation under conditions of uncertainty: the modulating role of incentives and social information. *Horm. Behav.* **57**, 368–374 (2010).
- Andrade, A., Paradis, A.-L., Rouquette, S. & Poline, J.-B. Ambiguous results in functional neuroimaging data analysis due to covariate correlation. *Neuroimage* **10**, 483–486 (1999).
- Wilson, R. C. & Niv, Y. Is model fitting necessary for model-based fMRI? *PLoS Comput. Biol.* **11**, e1004237 (2015).

## Reporting Summary

Nature Research wishes to improve the reproducibility of the work that we publish. This form provides structure for consistency and transparency in reporting. For further information on Nature Research policies, see [Authors & Referees](#) and the [Editorial Policy Checklist](#).

### Statistics

For all statistical analyses, confirm that the following items are present in the figure legend, table legend, main text, or Methods section.

n/a Confirmed

- The exact sample size ( $n$ ) for each experimental group/condition, given as a discrete number and unit of measurement
- A statement on whether measurements were taken from distinct samples or whether the same sample was measured repeatedly
- The statistical test(s) used AND whether they are one- or two-sided  
*Only common tests should be described solely by name; describe more complex techniques in the Methods section.*
- A description of all covariates tested
- A description of any assumptions or corrections, such as tests of normality and adjustment for multiple comparisons
- A full description of the statistical parameters including central tendency (e.g. means) or other basic estimates (e.g. regression coefficient) AND variation (e.g. standard deviation) or associated estimates of uncertainty (e.g. confidence intervals)
- For null hypothesis testing, the test statistic (e.g.  $F$ ,  $t$ ,  $r$ ) with confidence intervals, effect sizes, degrees of freedom and  $P$  value noted  
*Give  $P$  values as exact values whenever suitable.*
- For Bayesian analysis, information on the choice of priors and Markov chain Monte Carlo settings
- For hierarchical and complex designs, identification of the appropriate level for tests and full reporting of outcomes
- Estimates of effect sizes (e.g. Cohen's  $d$ , Pearson's  $r$ ), indicating how they were calculated

*Our web collection on [statistics for biologists](#) contains articles on many of the points above.*

### Software and code

Policy information about [availability of computer code](#)

Data collection

Presentation 17.0, MATLAB 2014b

Data analysis

MATLAB 2016b, R Studio 1.1.414, SPM12

For manuscripts utilizing custom algorithms or software that are central to the research but not yet described in published literature, software must be made available to editors/reviewers. We strongly encourage code deposition in a community repository (e.g. GitHub). See the Nature Research [guidelines for submitting code & software](#) for further information.

### Data

Policy information about [availability of data](#)

All manuscripts must include a [data availability statement](#). This statement should provide the following information, where applicable:

- Accession codes, unique identifiers, or web links for publicly available datasets
- A list of figures that have associated raw data
- A description of any restrictions on data availability

The data that support the findings of this study are available upon reasonable request.

### Field-specific reporting

Please select the one below that is the best fit for your research. If you are not sure, read the appropriate sections before making your selection.

- Life sciences       Behavioural & social sciences       Ecological, evolutionary & environmental sciences

For a reference copy of the document with all sections, see [nature.com/documents/nr-reporting-summary-flat.pdf](https://www.nature.com/documents/nr-reporting-summary-flat.pdf)

# Life sciences study design

All studies must disclose on these points even when the disclosure is negative.

Sample size	<p>The sample size of the current study was determined prior to data collection and was detailed as follows:</p> <ol style="list-style-type: none"> <li>1. Sample size estimation for the fMRI experiment. The sample size of the fMRI study was determined prior to data collection. We conducted sample size estimation using G*Power 3.1 (Faul et al., 2007) to determine the number of participants sufficient to detect a reliable effect. Based on an estimated average small-to-medium effect size of oxytocin effect on social behaviors (Cohen's <math>d = 0.28</math>, Walum et al., 2016). 104 participants were needed to detect a significant effect (<math>\alpha = 0.05</math>, <math>\beta = 0.80</math>, two-by-two mixed ANOVA interaction effects). We planned to recruit 125 participants (assuming 10-20% participants would be removed from the fMRI data analysis due to excessive head movement). In the end, we recruited 127 participants because the 41th and 42th participants did not complete the experiment due to technical issues during scanning. For comparison, we also considered the 58 oxytocin-fMRI studies published at the time we initiated our experiment in June 2015, of which 23 employed between-subject design recruiting healthy individuals. On average, the sample size was 50.89 in total, 25.82 for the placebo group and 25.47 for the oxytocin group. Thus, our planned sample size of 125 participants was a decent sample size compared to the average across oxytocin-fMRI studies. Moreover, the sample size of 116 participants (after removal of subjects due to technical issues and excessive head movement) was adequate to reveal reliable effects, exceeding the 104 participants needed for 80% power.</li> <li>2. Sample size estimation for the oxytocin replication experiment. We conducted an additional behavioral experiment for the replication of the oxytocin effect using a double-blind, randomized, placebo-controlled, within-subjects crossover design. The sample size was predetermined based on the effect size (Cohen's <math>d = 0.45</math>) from our original finding in the fMRI study. The G*Power calculation suggested that 40 participants (20 for each group) were required to detect a reliable effect (<math>\alpha = 0.05</math>, <math>\beta = 0.80</math> for a within (oxytocin vs. placebo)-between (prosocial vs. individualist) interaction). To obtain a better sense of the robustness of the original findings, we doubled the estimated sample size, aiming to enroll 40 participants per group, with corresponding power equal to 98%. We replicated the selective oxytocin effects on promoting prosociality (i.e., <math>\phi</math>) in individualists in the whole sample (40 prosocials and 40 individualists), as well as in the first 20 prosocials and 20 individualists (as estimated by the G*Power analysis). 140 males (mean age, <math>22.33 \pm 3.35</math> years) were invited to a behavioral session to identify their disposition in social value orientation. Among these, 82 participants were qualified and willing to participate in the oxytocin experiment (at least 7 days after the first behavioral session). Two participants did not show up for the second session. Thus, 80 participants (40 prosocials, mean age, <math>22.08 \pm 3.47</math> years; 40 individualists; mean age, <math>21.54 \pm 2.42</math> years) were included in the final data analysis.</li> </ol> <p>Reference. Faul, F., Erdfelder, E., Lang, A. G. &amp; Buchner, A. G*Power 3: a flexible statistical power analysis program for the social, behavioral, and biomedical sciences. <i>Behav Res methods</i> 39, 175-191 (2007). Walum, H., Waldman, I.D. &amp; Young, L.J. Statistical and Methodological Considerations for the Interpretation of Intranasal Oxytocin Studies. <i>Biol. Psychiatry</i>. 79, 251-257 (2016).</p>
Data exclusions	<p>The exclusion criteria were established prior to data analysis based on previously published papers in the field. Subjects with poor performance and excessive head motion during scanning would be excluded, which was in line with with a majority of fMRI studies.</p> <ol style="list-style-type: none"> <li>1. Behavior: Button responses were recorded for each trial. Responses that were not recorded within four seconds were discarded, based on the time limit of jitter.</li> <li>2. fMRI: Scans that exceeded 3 mm of intravolume motion were excluded in line with Power et al., 2012's instruction.</li> </ol> <p>Reference. Power, J. D., Barnes, K. A., Snyder, A. Z., Schlaggar, B. L., &amp; Petersen, S. E. Spurious but systematic correlations in functional connectivity MRI networks arise from subject motion. <i>Neuroimage</i>, 59, 2142-2154 (2012).</p>
Replication	<ol style="list-style-type: none"> <li>1. We had a post-scan behavioral experiment on the same participants went through fMRI studies - the results are largely the same.</li> <li>2. Before the actual experiment, we have recruited another independent sample of participants (<math>n=60</math>) to perform a very similar task, the results are very similar as the main finding.</li> <li>3. We have run two additional experiments (<math>N = 315</math> and <math>N = 140</math>) with a revised experimental design. The first additional study with a large sample size (<math>N = 315</math>) provides a replication for our winning social referent point model. The second additional study was an oxytocin experiment that replicated the selective oxytocin effect in prosocials and individualists and the winning model again (<math>N = 80</math> males for a within-subject, placebo-controlled design with oxytocin challenge, 40 prosocials and 40 individualists, 140 males screened for social value orientation). The two additional experiments were both run on a modified design that improved the ability to distinguish between different models. We replicated the effects reported in the original manuscript across both samples using the improved design. All results are reported in the main text.</li> </ol>
Randomization	<p>Participants recruited in the fMRI experiment were randomly assigned to the intranasal administration of oxytocin or placebo in a double-blind placebo-controlled between-subjects design.</p> <p>Oxytocin-replication experiment. We conducted an additional behavioral experiment for the replication of the oxytocin effect using a double-blind, randomized, placebo-controlled, within-subjects crossover design. The order of oxytocin and placebo treatment was counterbalanced across participants.</p>
Blinding	<p>The oxytocin-fMRI and oxytocin-replication experiments were double-blind, i.e., both participants and experimenters were blind to experimental conditions (both treatment and social disposition conditions). Data analysis was not performed blind to the conditions of the experiments.</p>

## Reporting for specific materials, systems and methods

We require information from authors about some types of materials, experimental systems and methods used in many studies. Here, indicate whether each material, system or method listed is relevant to your study. If you are not sure if a list item applies to your research, read the appropriate section before selecting a response.

## Materials &amp; experimental systems

n/a	<input type="checkbox"/> Involved in the study
<input checked="" type="checkbox"/>	<input type="checkbox"/> Antibodies
<input checked="" type="checkbox"/>	<input type="checkbox"/> Eukaryotic cell lines
<input checked="" type="checkbox"/>	<input type="checkbox"/> Palaeontology
<input checked="" type="checkbox"/>	<input type="checkbox"/> Animals and other organisms
<input type="checkbox"/>	<input checked="" type="checkbox"/> Human research participants
<input checked="" type="checkbox"/>	<input type="checkbox"/> Clinical data

## Methods

n/a	<input type="checkbox"/> Involved in the study
<input checked="" type="checkbox"/>	<input type="checkbox"/> ChIP-seq
<input checked="" type="checkbox"/>	<input type="checkbox"/> Flow cytometry
<input type="checkbox"/>	<input checked="" type="checkbox"/> MRI-based neuroimaging

## Human research participants

Policy information about [studies involving human research participants](#)

## Population characteristics

Oxytocin fMRI experiment: There were 282 male college students (mean age=22.3 ± 2.12 years) that participated in this study as paid volunteers. 127 participants were qualified and willing to participate in the fMRI experiment. Two participants (1.6%) were excluded due to technical issues during scanning, leaving 125 participants in the behavioral analysis. An additional 9 participants (7.2%) were excluded from further fMRI analysis due to excessive head movement during scanning (> 3 mm), leaving 116 participants for fMRI data analysis. In the end, there were 60 prosocials including 30 administered placebo (mean age, 22.7 ± 2.61 years) and 30 administered oxytocin (mean age, 21.8 ± 2.38 years), and 56 individualists including 30 administered placebo (mean age, 23.0 ± 2.29 years) and 26 administered oxytocin (mean age, 22.5 ± 3.03 years) in the formal fMRI data analysis. Prosocials and individualists receiving oxytocin or placebo were matched on state and trait anxiety, depression, subjective well-being and happiness ratings (all  $p > 0.05$  on both the main and interaction effects of Treatment and Social Disposition; Supplementary Table 3a).

Oxytocin-replication experiment: 140 males (mean age, 22.33 ± 3.35 years) were invited to a behavioral session to identify their disposition in social value orientation. Among these, 82 participants were qualified and willing to participate in the oxytocin experiment (at least 7 days after the first behavioral session). Two participants did not show up for the second session. Thus, 80 participants (40 prosocials, mean age, 22.08 ± 3.47 years; 40 individualists; mean age, 21.54 ± 2.42 years) were included in the final data analysis. Prosocials and individualists were matched on state and trait anxiety, depression, subjective well-being and happiness ratings (all  $p > 0.05$  on both the main and interaction effects of Treatment and Social Disposition; Supplementary Table 3b).

Online-replication experiment: We conducted an online experiment with a large sample ( $n = 315$ , 132 males, 160 prosocials, mean age = 22.40 ± 3.27; 155 individualists, mean age = 22.48 ± 3.30) to provide a replication for our finding that the social reference model outperforms other models. (82 female, age=22.40±3.27, SVO score=9.16±7.74) and 155 individualists (101 female, age=22.48±3.30, SVO score= 33.62±5.63). Prosocials and individualists did not differ in their ratings on the first impression, likeability and attractiveness of the online partner (independent-samples  $t$  test, impression:  $t_{313} = 1.03$ ,  $p = 0.305$ ; likeability:  $t_{313} = 0.98$ ,  $p = 0.328$ ; attractiveness:  $t_{313} = 0.73$ ,  $p = 0.465$ ).

## Recruitment

Oxytocin fMRI experiment: 282 male college students were recruited in this study as paid volunteers through on campus flyer recruitment. We first measured participant's disposition in social value orientation in the behavioral session. Among these, 127 participants were qualified and willing to participate in the fMRI experiment.

Oxytocin-replication experiment: We recruited 140 males through on campus flyer recruitment to a behavioral session to identify their disposition in social value orientation. Among these, 82 participants were qualified and willing to participate in the oxytocin experiment.

Online-replication experiment: This is an on-line behavioral study with 315 participants, which were recruited on Qualtrics.

Although previous work has found demographic effects of recruiting volunteers into experiments that they may have less income and more leisure time (Cleave et al., 2013), our subject recruitment was based on the scores of social value orientation of randomly recruited participants. Moreover, the within-subject design of the oxytocin replication experiment, as well as the randomization process also minimize the influence of population's difference.

Ref. Cleave, B. L., Nikiforakis, N., & Slonim, R. Is there selection bias in laboratory experiments? The case of social and risk preferences. *Experimental Economics*, 16, 372-382 (2013).

## Ethics oversight

The experimental protocol was in line with the standards of the Declaration of Helsinki and approved by the research ethics committee at the State Key Laboratory of Cognitive Neuroscience and Learning, Beijing Normal University (Beijing, China).

Note that full information on the approval of the study protocol must also be provided in the manuscript.

## Magnetic resonance imaging

## Experimental design

## Design type

task fMRI, event-related design

## Design specifications

2 scanning sessions per participant; 90 trials per session; trial length ranged from 7 to 12 seconds; inter-trial interval length ranged from 4 to 6 seconds.

Behavioral performance measures Participants evaluated their preferences for a monetary allocation by button press in each trial. Button responses were recorded for each trial. Responses that were not recorded within four seconds were discarded. The preferences and decision times were measured.

## Acquisition

Imaging type(s) functional, structural

Field strength 3 Tesla

Sequence & imaging parameters Whole-brain imaging data was collected on a GE 3-Tesla MR scanner with a standard head coil (HDx, Signa MR 750 System; GE Healthcare, Milwaukee, WI). Functional images were collected using an echo-planar imaging sequence (axial slices, 32; slice thickness, 4 mm; gap, 1 mm; TR, 2000 ms; TE, 30 ms; voxel size,  $3.75 \times 3.75 \times 5$  mm; flip angle,  $90^\circ$ ; FOV,  $240 \times 240$  mm; and 285 volumes for each session, two sessions in total). Structural images were acquired through 3D sagittal T1-weighted magnetization-prepared rapid gradient echo (180 slices; TR, 8.208 ms; TE, 3.22 ms; slice thickness, 1 mm; voxel size,  $0.47 \times 0.47 \times 1.0$  mm<sup>3</sup>; flip angle,  $12^\circ$ ; inversion time, 450 ms; FOV,  $240 \times 240$  mm).

Area of acquisition Whole brain; each volume comprised 32 axial slices collected in an interleaved-ascending manner and parallel to the AC-PC line.

Diffusion MRI  Used  Not used

## Preprocessing

Preprocessing software Brain imaging data was preprocessed using Statistical Parametric Mapping (SPM12; <http://www.fil.ion.ucl.ac.uk/spm/>). The first 5 functional images from each session were discarded for signal equilibrium and participants' adaptation to scanning noise. Remaining images were corrected for slice acquisition timing and realigned for head motion correction. Subsequently, functional images were coregistered to each participant's grey matter image segmented from corresponding high-resolution T1-weighted image, then spatially normalized into a common stereotactic Montreal Neurological Institute (MNI) space and resampled into 2-mm isotropic voxels. Finally, images were smoothed by an isotropic 3D Gaussian kernel with 8-mm full-width at half-maximum.

Normalization We used the 'Old normalise' template from SPM12 which, according to the manual (<http://www.fil.ion.ucl.ac.uk/spm/doc/manual.pdf>), states the following: "The first step of the normalisation is to determine the optimum 12-parameter affine transformation. Initially, the registration is performed by matching the whole of the head (including the scalp) to the template. Following this, the registration proceeded by only matching the brains together, by appropriate weighting of the template voxels. This is a completely automated procedure (that does not require "scalp editing") that discounts the confounding effects of skull and scalp differences. A Bayesian framework is used, such that the registration searches for the solution that maximises the a posteriori probability of it being correct. i.e., it maximises the product of the likelihood function (derived from the residual squared difference) and the prior function (which is based on the probability of obtaining a particular set of zooms and shears). The affine registration is followed by estimating nonlinear deformations, whereby the deformations are defined by a linear combination of three dimensional discrete cosine transform (DCT) basis functions. The default options result in each of the deformation fields being described by 1176 parameters, where these represent the coefficients of the deformations in three orthogonal directions. The matching involved simultaneously minimising the membrane energies of the deformation fields and the residual squared difference between the images and template(s)."

Normalization template Images were transformed to conform to the default T1 Montreal Neurological Institute (MNI) brain interpolated to  $3 \times 3 \times 3$  mm.

Noise and artifact removal Scans that exceeded 3 mm of intravolume motion were excluded

Volume censoring We used the ArtRepair toolbox to remove artifacts. Values for repaired scans were imputed and dewighted by interpolating between the nearest non-repaired scans.

## Statistical modeling & inference

Model type and settings mass univariate; level 1: fixed effects, high-pass filter with cutoff period of 128 s was used; level 2: random effects

Effect(s) tested At first level, we created parametric regressors that were associated with the value distance or value difference between self and other, at the monetary outcome-pair presentation to search for brain regions that encoded the subjective distance in social value representation. In the fMRI analysis, we included 10 GLM models: a social value distance from an individual-specific reference-point (i.e.,  $1 - \cos(\theta(t) - \phi)$ ,  $\theta(t)$  is the angle of a potential allocation at trial  $t$  and  $\phi$  is the individual-specific reference-point derived from our social reference model), an egocentric reference (i.e.,  $\cos(\theta(t))$ ), an allocentric reference (i.e.,  $\sin(\theta(t))$ ), an objective equality reference-point (i.e.,  $\cos(\theta(t) - 45^\circ)$ ), monetary outcome for the self (i.e.,  $\$Self$ ), monetary outcome for the partner (i.e.,  $\$Other$ ), absolute value difference ( $|\$Self - \$Other|$  or advantageous (i.e.,  $\max(0, \$Self - \$Other)$ ) or disadvantageous inequality aversion (i.e.,  $\max(0, \$Other - \$Self)$ ) separately, or with preference rating as parametric modulator in the GLM.

At second level, Coefficients for each regressor were estimated for each participant using maximum likelihood estimates to account for serial correlations in the data. Statistical significance was determined at the group level using a random-effects analysis. Significant clusters from all 2nd-level analyses were determined using a height threshold of  $P < 0.001$  and an extent threshold of  $P < 0.05$  with family-wise error (FWE) correction. We also applied voxelwise inference



using FWE-corrected threshold of  $P = 0.05$  on the whole-brain analysis, given recently recognized concern over clusterwise inference. For the relationship between value distance ( $1 - \cos(\theta(t) - \phi)$ ) and neural responses during monetary outcome pair presentation, the peak voxels in right amygdala survived voxelwise FWE correction ( $P = 0.02$ ).

Specify type of analysis:  Whole brain  ROI-based  Both

Anatomical location(s)

All ROI analyses were employed on regions defined anatomically. Amygdala ROIs are defined based on AAL bilateral anatomical mask. LOFC are defined based on based on Neubert et al. (2014), combining connectivity-based parcellations 8-11, which includes all of right IOFC.

Ref. Neubert, F.X., Mars, R.B., Thomas, A.G., Sallet, J. & Rushworth, M.F. Comparison of human ventral frontal cortex areas for cognitive control and language with areas in monkey frontal cortex. *Neuron* 81, 700-713 (2014).

Statistic type for inference  
(See [Eklund et al. 2016](#))

Statistical significance was determined at the group level using a random-effects analysis. Significant clusters from second-level analyses were determined using a height threshold of  $P < 0.001$  and an extent threshold of  $P < 0.05$  with cluster-based family-wise error (FWE) correction. We also applied voxelwise inference using the FWE-corrected threshold of  $P = 0.05$  on the whole-brain analysis, given recent concern over cluster-wise inferences. For the relationship between value distance ( $1 - \cos(\theta(t) - \phi)$ ) and neural responses during monetary outcome-pair presentation, the peak voxels in right amygdala survived voxelwise FWE correction ( $P = 0.02$ ).

Correction

Significant clusters from second-level analyses were determined using a height threshold of  $P < 0.001$  and an extent threshold of  $P < 0.05$  with cluster-based family-wise error (FWE) correction. We also applied voxelwise inference using the FWE-corrected threshold of  $P = 0.05$  on the whole-brain analysis, given recent concern over cluster-wise inferences. For the relationship between value distance ( $1 - \cos(\theta(t) - \phi)$ ) and neural responses during monetary outcome-pair presentation, the peak voxels in right amygdala survived voxelwise FWE correction ( $P = 0.02$ ).

## Models & analysis

- n/a | Involved in the study
- Functional and/or effective connectivity
- Graph analysis
- Multivariate modeling or predictive analysis

Functional and/or effective connectivity

Functional connectivity was measured. We performed a generalized PPI analysis with anatomically defined bilateral amygdala as the seed region at the whole-brain level.